

1 **Detecting the resilience of soil moisture dynamics to drought** 2 **periods as function of soil type and climatic region**

3 Nedal Aqel¹, Jannis Groh^{2,3}, Lutz Weihermüller², Ralf Gründling⁴, Andrea Carminati¹, Peter
4 Lehmann¹

5 ¹Physics of Soils and Terrestrial Ecosystems, ETH Zurich, Zurich, Switzerland

6 ²Institute of Bio- and Geoscience IBG-3: Agrosphere, Forschungszentrum Jülich GmbH, Jülich, Germany

7 ³Biogeochemistry and Gas Fluxes, Leibniz Institute for Agricultural and Landscape Research (ZALF),
8 Müncheberg, Germany

9 ⁴Department of Soil System Science, Helmholtz-Zentrum für Umweltforschung GmbH – UFZ, Halle, Germany

10 *Corresponding author, nedal.aqel@usys.ethz.ch, Universitätsstrasse 16, 8092 Zurich, Switzerland

11 **Abstract**

12 Abrupt changes in climatic conditions and land management can cause permanent shifts in soil
13 hydraulic response to climatic inputs, impacting soil functions and established soil–climate interactions.

14 To quantify the resilience of soil water content dynamics after abrupt changes in environmental
15 conditions, we present a model framework combining a neural network with seasonal trend analysis

16 (STL). Using data from a series of ~~lysimeters from lysimeter form~~ the TERrestrial ENvironmental

17 ~~Observatories~~Observatories (TERENO) - SOILCan lysimeter network, we identified changes in ~~the~~

18 ~~response of~~ soil water content ~~responses~~ after an extremely hot and dry summer in Germany in ~~the year~~

19 2018. The model incorporates meteorological variables decomposed into seasonal and long-term

20 components along with a categorical indicator of current moisture conditions. It is trained on data from

21 a reference site with stable soil water content response and applied to lysimeters from multiple origins

22 exposed to contrasting climates. By analysing annual residual patterns—particularly mean bias over

23 time—soil water content state dynamics is classified as ‘stable’, ‘resilient’, or ‘changed’, reflecting

24 whether the system maintains, recovers, or diverges from its original state. We found that soils preserve

25 the response function to environmental forcing under typical conditions but exhibit ~~structural change~~

26 ~~changes in hydraulic behaviour~~ when relocated to new environments, even when soil texture remains

27 constant. The proposed method offers a scalable and non-invasive tool for tracking changes in the

28 response of soil water content to climatic change and provides early indicators of changes in essential

29 soil functions and soil health status.

1. Introduction

Soil water content plays a fundamental role in hydrological processes and land–atmosphere interactions, governing the exchange of water and energy at the Earth’s surface (Seneviratne et al., 2010; Sun et al., 2025). It regulates key hydrological functions, including infiltration, runoff generation, evapotranspiration, and groundwater recharge. Through these processes, soil water content influences water availability, ecosystem productivity, and climatic conditions across local to global scales (Bogena et al., 2015; Fatichi et al., 2020). Soil water content status and related soil environmental conditions change with short- and long-term atmospheric processes. This response of soil water content to atmospheric conditions, which we define as ‘soil water content response function’, determines, for example, if anaerobic conditions are inhibited after heavy rainfall (by fast percolation to deeper soil layers) and if enough water remains available after dry periods for plant growth, temperature regulation, and chemical reactions. In short, the soil water content response function is ~~a dominant factor~~ an indicator of the near-surface hydraulic functioning and land–atmosphere exchange processes, which are relevant for several soil health-status-related processes such as infiltration efficiency, surface aeration, and runoff generation. This response function is shaped by soil formation processes and reflects adaptation to the dominant climatic conditions (Kuzyakov and Zamanian, 2019; Sainju et al., 2022; ~~Al-Shammary et al., 2025~~). Accordingly, a change in the response function after extreme climatic events is likely to imply a change in soil health.

In the core of this study is the question how changes in the soil water content response function, and thus in soil properties and health, can be detected. The standard approach to determine the response function is to apply physically based models, for example by inverse modelling of soil water content dynamics under varying boundary conditions (Šimůnek et al., 2016). These models require detailed knowledge of soil hydraulic properties and extensive calibration, limiting their generalization beyond the spatial scale and the local conditions used in the calibration process (~~(O., 2020;~~ Lehmann et al., 2020; O. & Orth, 2021). Additionally, ~~such approaches~~ soil hydraulic parameters for physically based models are typically destructive usually obtained through soil sampling or sensor installation, both of which disturb the soil structure, limiting the ~~options of conducting a~~ feasibility of repeated

57 [measurements for long-term](#) time-series analysis. Moreover, these models typically assume static soil
58 characteristics, failing to adequately represent structural changes in soil properties—[such as](#)
59 compaction, degradation, or organic matter loss—[that can substantially alter hydraulic behaviour](#)
60 over time (Fatichi et al., 2020; Melsen & Guse, 2021; Wankmüller et al., 2024). Most of the models
61 also neglect or oversimplify the hysteretic nature of the soil water retention curve, as well as seasonal
62 changes in soil hydraulic properties that can substantially alter infiltration, drainage, and plant water
63 availability (Aqel et al., 2024; Hannes et al., 2016; Herbrich & Gerke, 2017). Therefore, we used a non-
64 invasive approach based on neural networks as discussed below.

65 In recent years, artificial intelligence (AI), particularly neural networks, has emerged as a promising
66 alternative for modelling complex hydrological processes (Reichstein et al., 2019). These data-driven
67 models have demonstrated the capacity to learn nonlinear relationships directly from observational
68 datasets without relying heavily on explicit physical equations (Kratzert et al., 2019; Mosavi et al.,
69 2018; Shen et al., 2018). Within soil hydrology, neural networks have been used to characterise
70 hysteretic soil–water behaviour from training data, improving the representation of wetting–drying
71 cycles without explicit hysteresis parameterisation (Aqel et al., 2024). They have also been applied to
72 soil-moisture time-series modelling using Long Short-Term Memory (LSTM) networks with recurrent
73 architectures suited to capture long-range temporal dependencies (Liu et al., 2023; O. & Orth, 2021).
74 Across diverse hydro-climatic regimes, LSTM have been shown to effectively learn nonlinear
75 relationships between climatic inputs and soil water content, often matching or surpassing traditional
76 physically based approaches and demonstrating strong generalisation (Kratzert et al., 2019; J. Liu et al.,
77 2022, 2023; O. & Orth, 2021).

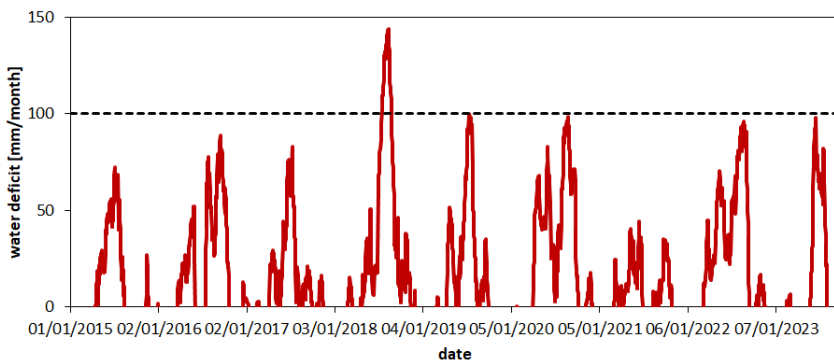
78 Independent of the chosen modelling approach, these models ignore that the soil water content response
79 function (i.e., the variations in soil water content following changes in atmospheric conditions) can
80 change at [a larger time scale](#). Experimental studies have shown that extreme events such as drought can
81 induce persistent shifts in soil water content dynamics, potentially leading to alternative stable states
82 [see \(Robinson et al., 2016\), Quintana et al., 2023 and the section on illustrative examples in Robinson](#)
83 [et al., 2019\)](#). Moreover, changes in land use—[such as forest conversion to agriculture or bare land](#)

84 ~~—~~alter soil hydraulic properties, with effects on infiltration, water retention, and saturated hydraulic
85 conductivity (Fu et al., 2021; Robinson et al., 2022). Considering that soil texture (particle-size
86 distribution) remains constant at time scales of decades, the changes in the response function are likely
87 to be related to changes in soil structure ~~primarily and associated hydraulic properties driven by~~
88 structural reorganization, wettability effects, root activity, or land-use changes rather than to textural
89 change.

90 Soil systems are subject to temporal change, yet models are often trained on historical datasets without
91 evaluating whether the system dynamics remain stable throughout the training period (Montanari et al.,
92 2013; Vaze et al., 2010). As a result, models may be applied to prediction settings where underlying
93 soil–climate interactions differ from those on which the model was trained. For example, a recent study
94 comparing different crop models using the TERENO-SOILCan set-up showed that predicting
95 agronomic and environmental variables under different climatic conditions to those represented in the
96 training datasets resulted in significant discrepancies between simulations and observations (Groh et
97 al., 2022). This underscores the critical need to assess whether site-specific representations of soil–
98 water behaviour remain valid over time (Hrachowitz et al., 2013) and highlight the need for more
99 adaptable modelling approaches under evolving environmental conditions (Blöschl et al., 2019; Milly
100 et al., 2008). ~~Considering these limitations, none of the discussed approaches can capture the change in~~
101 ~~the soil water content response function.~~ A recent modelling framework by Jarvis et al. (2024) takes a
102 major conceptual step forward by explicitly representing soil-structure dynamics and their feedback on
103 hydraulic behaviour. However, as the authors emphasize, such process-based models still depend on
104 detailed observational data to constrain temporal changes in structure and hydraulic properties.

105
106 To address this gap, the present study introduces a framework based on neural networks and seasonal
107 trend decomposition. ~~Specifically, we~~ This framework is applied to quantify ~~the change~~ changes in the
108 soil response function ~~after following~~ the 2018 summer drought ~~in summer, which was,~~ a Europe-wide
109 ~~event, but in Germany was particularly characterized by an~~ extreme combination of high temperatures
110 ~~and low~~ event. During this period, total precipitation in central Europe fell to the lowest percentiles

111 relative to the 1976–2005 reference distribution. In Germany, the summer of 2018 was characterised
112 by one of the warmest years on record and the lowest precipitation since 1881 (Xoplaki et al., 2025).
113 The response of soil water content on this drought will be analysed ~~for~~with a set of lysimeters. As shown
114 in Fig. 1 for one of the study sites, the monthly water deficit (potential evapotranspiration minus
115 precipitation) peaked in summer 2018 indicating the strong drought in this period.



116 **Figure 1** Variations in climatic conditions at Selhausen (SE) expressed as difference between potential
117 evapotranspiration (PET) and precipitation (P) cumulated over the precedent 30 days (one month). The extreme
118 summer 2018 is manifested by a maximum monthly deficit of ~150 mm. Details on the calculation of PET are
119 provided in section 2.1.1.
120

121 ~~The general objective of this study is thus to introduce a model framework to quantitatively detect~~
122 ~~changes in the soil water content response function and to classify the response as ‘stable’, ‘resilient’,~~
123 ~~or ‘changed’.~~

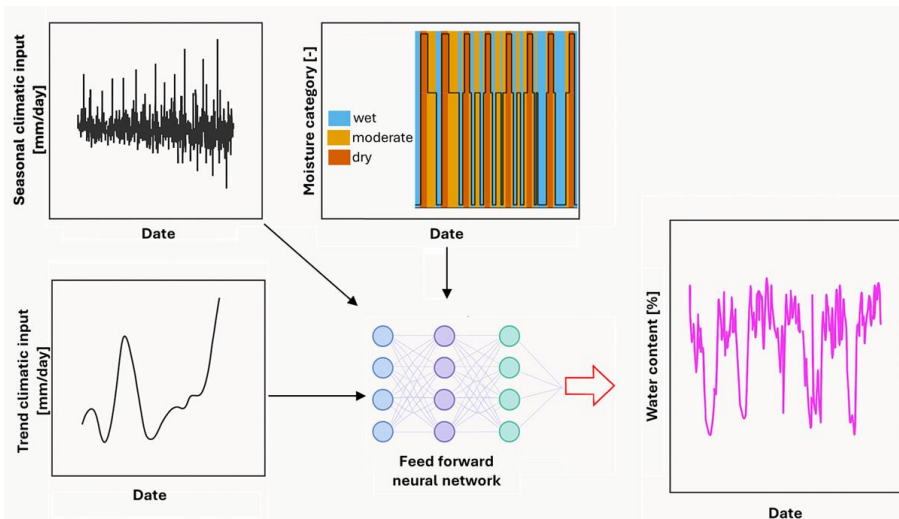
124 The general objective of this study is to introduce a model framework to quantitatively detect changes
125 in the soil water content response function and to classify the response as “stable”, “resilient”, or
126 “changed”. These terms are used here as operational classes describing the temporal behaviour of the
127 response function, rather than as formal system-level properties or metrics as defined in ecological and
128 complex systems theory. In that literature, resilience is commonly understood as a system property
129 reflecting the capacity to absorb disturbance and recover, while stability refers to the tendency of system
130 dynamics to remain close to a reference state or equilibrium (Holling, 1973). Resilience is often
131 discussed in relation to both resistance to perturbation and the subsequent recovery toward pre-
132 established levels. In the context of this study, “stable” denotes the validity of a single response function

133 ~~throughout the entire monitoring period. “Resilient” denotes a temporary deviation from this response~~
134 ~~function following an extreme event (summer 2018), followed by a return to the pre-event response~~
135 ~~within the observation window. In the third case, denoted here as “changed”, the response function at~~
136 ~~the end of the observation period remains distinct from the pre-2018 reference response. Whether such~~
137 ~~a change represents a persistent transition to an alternative response regime or a transient deviation with~~
138 ~~delayed recovery cannot be determined based on the available time series.~~

139
140
141 In principle, it would be possible to develop a quantitative framework to detect changes in the response
142 function exclusively based on experimental data of time series (without modelling~~es~~), for example by
143 the application of wavelet analysis (Ehrhardt et al., 2025). In this study, ~~however,~~ we ~~pursue~~adopt a
144 ~~different approach based on~~ predictive modelling ~~approach~~ in which ~~the temporal evolution of~~
145 ~~differences/deviations~~ between ~~measurements/observed~~ and ~~predictions/serves as an indicator of~~
146 ~~changes in the response function, yields both, accurate predictions of/simulated~~ soil water content
147 ~~dynamics (not in the focus of this study) and detection of/over time are used to identify~~ changes in the
148 ~~relationship between soil-climate and response function. While the model also produces predictions of~~
149 ~~soil water content dynamics,~~ prediction accuracy is not the primary objective; instead, model-data
150 ~~deviations are used to detect temporal drift in soil water response behaviour. The overall level of~~
151 ~~dynamic agreement is summarized using Nash-Sutcliffe efficiency, while the detection and~~
152 ~~classification of changes rely on the temporal evolution of mean bias, as described in Section 2.5.~~

153 2. Material and Methods

154 We developed a data-driven modelling framework that combines time-series decomposition of climatic
155 inputs with a feed-forward neural network to predict the daily soil water content (Fig. 2).



156
 157 **Figure 2** Schematic overview of the modelling framework for daily soil water content prediction. Input features
 158 include the analysis of a climatic variable (top left), its long-term trend component (bottom left), and the
 159 categorical soil water content state ('wet', 'moderate', 'dry'; top middle). These features, derived from observed
 160 data, are used to train a feed-forward neural network (centre), which outputs daily predictions of volumetric
 161 water content (right). The model thus captures temporal soil water content dynamics based on structured climate
 162 signals and categorical conditions.

163 The approach explicitly incorporates precipitation_r (**P**), potential evapotranspiration_r (**PET**), and their
 164 difference (climatic water balance) as primary inputs. Each of these climate drivers was decomposed
 165 into seasonal variations and long-term trend components using Seasonal-Trend decomposition (STL)
 166 and was included as a separate feature in the model (Boergens et al., 2024; Cleveland et al., 1990). **The**
 167 **daily climatic water balance (WB) was included to reflect the net difference between P and PET, serving**
 168 **as a proxy for wetting or drying conditions. Positive values indicate potential moisture accumulation**
 169 **(e.g., during rainfall-dominated periods), while negative values reflect high evaporative demand and**
 170 **drying conditions (e.g., during hot, dry spells). Including the WB helps the model to distinguish humid**
 171 **periods from dry ones. By providing WB alongside P and PET, the model can learn both the individual**
 172 **and combined effects of precipitation and evaporative demand on soil water content dynamics (Brocca**
 173 **et al., 2010; Uber et al., 2018). For example, it can infer that 10 mm of P during a high-PET summer**
 174 **day (low positive or negative WB) is less likely to increase soil water content than the same P on a cool,**
 175 **low-PET day (high positive WB).**

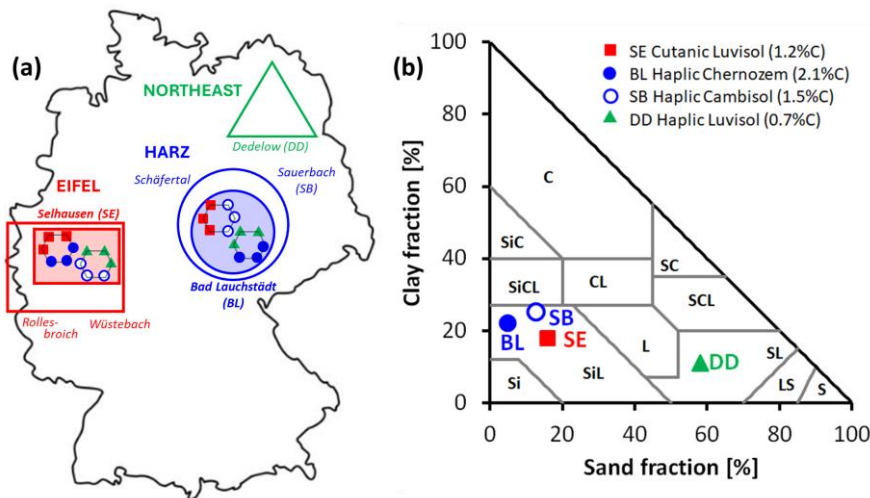
176 The input features also included a categorical moisture class (type) that reflects the expected current
177 soil water condition ('wet', 'moderate', 'dry'). This design reflects the understanding that changes in
178 climate - such as shifts in rainfall and evaporative demand - substantially affect soil water availability
179 and fluxes (Vereecken et al., 2022). The methodology is detailed in the following sections, which
180 consists of five key steps: selecting study sites and datasets collected in contrasting hydro-climatic
181 conditions (subsection 2.1), preprocessing the data and extracting meaningful signals features including
182 STL (subsection 2.2), constructing and training a neural network model on a reference dataset
183 (subsection 2.3), generating soil water content predictions for independent (non-training) sites using the
184 trained model (subsection 2.4), evaluating the model's performance with statistical metrics (subsection
185 2.5), and physical consistency checks (subsection 2.6).

186 2.1 Study Sites and Data Selection

187 2.1.1 Lysimeter Network TERENO SOILCan

188 The study was conducted using lysimeter data from the TERENO-SOILCan lysimeter network in
189 Germany (Pütz et al., 2016) with a focus on two locations: Bad Lauchstädt (BL) and Selhausen (SE)
190 (Fig. 3). These sites were selected for their contrasting climatic regimes and the specific set-up of
191 lysimeters, providing a natural experiment on how climate variability influences soil hydrological
192 behaviour for a variety of soils. The TERENO-SOILCan lysimeters were moved between and within
193 observatories according to a modified space-for-time approach, to expose them to different climates
194 (Groh et al. 2020). This allows us to compare the ecosystem response of the same soil, but under
195 different climatic conditions. Selhausen is characterized by a humid, Atlantic-influenced climate
196 (annual precipitation around 720 mm and mean air temperature around 10 °C), whereas Bad Lauchstädt
197 represents a drier, more continental climate (annual precipitation roughly 487 mm and mean air
198 temperature approximately 8.8 °C); both climate descriptions ~~are~~were based on Pütz et al. (2016). Long-
199 term observations ~~confirm~~confirmed that Bad Lauchstädt experiences significantly lower rainfall and
200 higher evaporative demand than Selhausen, yielding a higher aridity index (ratio of potential
201 evapotranspiration to precipitation) and more pronounced dry spells in the growing season. By
202 including both, a wetter site (Selhausen) and a drier site (Bad Lauchstädt), the model is evaluated under

203 distinctly different moisture regimes, which is critical for testing the generality of the approach and to
 204 separate between climatic and soil type effects. For each lysimeter station (Bad Lauchstädt and
 205 Selhausen), 12 lysimeters (1 m² surface area, 1.5 m depth) arranged in hexagons with 6 lysimeters
 206 around a service well were included in the analysis to monitor soil water content along with
 207 meteorological variables. In this study, lysimeters ~~are~~ were not used for drainage or storage estimates,
 208 but rather as instruments providing long-term, high-resolution time series of soil water content and
 209 matric potential under field conditions. The lysimeters contain undisturbed soil columns collected at
 210 four different locations (see Fig. 3a), each with three replicates (Pütz et al., 2016) and were managed as
 211 arable land under crop rotation. Note that all lysimeters were collected in the field and transported to
 212 the lysimeter station (Pütz et al., 2016) such that no differences regarding packing and boundary effect
 213 can be expected. While fertilization practices differed regionally until spring 2019, the overall
 214 management concept was comparable, ensuring that differences in water dynamics can be attributed to
 215 changes in the climate and soil rather than the management (Pütz et al., 2016).



216
 217 **Figure 3** Overview of the study area with site locations, topsoil texture, and soil origin. (a) The TERENO-
 218 SOILCan network contains lysimeters from four climatic regions (different symbols and colours in map). Our
 219 analysis focuses on the TERENO–SOILCan sites Selhausen (SE) and Bad Lauchstädt (BL), located in the
 220 Eifel/lower rhine valley and Harz/central German lowland observatory of TERENO, respectively, because at both
 221 sites lysimeter clusters were built (represented by shaded areas and hexagons), collecting large soil columns from
 222 four distinct source regions (i.e., Dedelow (DD), Bad Lauchstädt (BL), Sauerbach (SB), and Selhausen (SE)). (b)

223 *The analysed soil horizons (10 cm depth) cover two textural classes, shown in the USDA soil texture triangle,*
224 *assigned to four different soil types and a range of soil organic carbon contents (SOC) (numbers in the legend).*

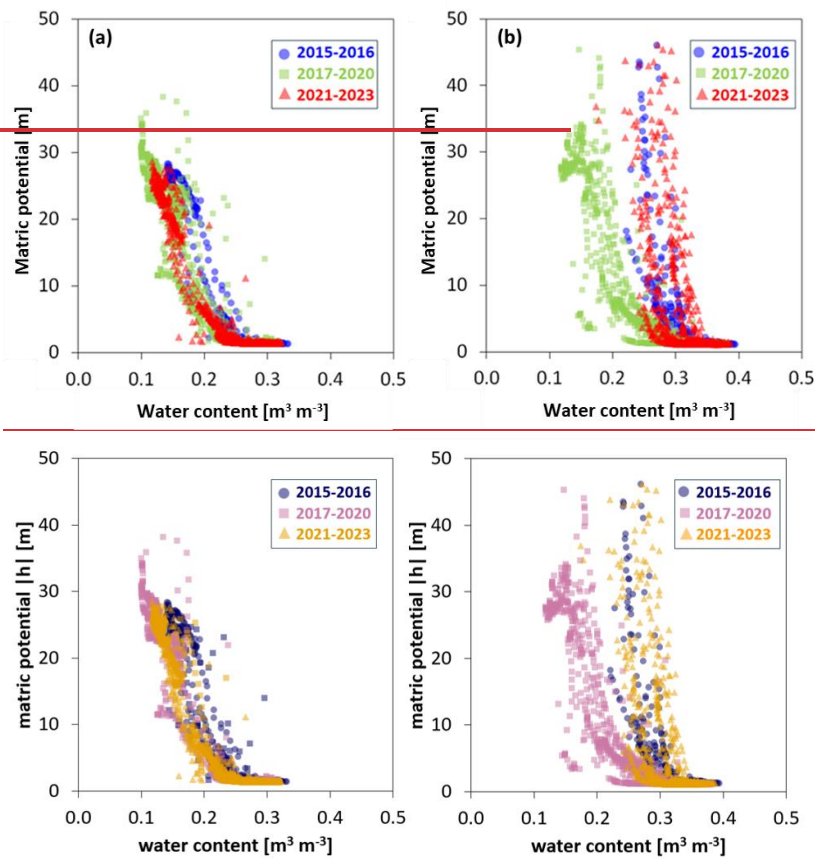
225 To investigate the effects of climate on soil water dynamics, daily time series of precipitation (P),
226 potential evapotranspiration (PET), matric potential, and volumetric soil water content (used as the
227 target variable) were compiled. ~~P~~Precipitation at Selhausen was measured at the on-site SOILCan
228 weather station, while for Bad Lauchstädt it was taken from the nearest long-term monitoring station
229 operated by the Deutscher Wetterdienst (Leipzig/Halle, ID 2932; DWD Climate Data Center, 2025).

230 PET was calculated with the FAO-56 Penman–Monteith model (Allen et al., 2006), using measured
231 meteorological variables (air temperature, air pressure, relative humidity, radiation, and wind speed)
232 according to SOILCan protocols (Pütz et al., 2016; Groh et al., 2020). In this context, the reference
233 evapotranspiration (ET_0) calculated with the Penman–Monteith model for a clipped grass surface
234 (FAO-56) is used as a proxy for potential evapotranspiration (PET), representing the site-independent
235 atmospheric evaporative demand. Soil matric potential was measured using MPS-1 sensors (Decagon
236 Devices Inc., Pullman, WA, USA), and volumetric soil water content was measured with time-domain
237 reflectometry probes (CS610, Campbell Scientific, North Logan, UT, USA). The observational record
238 spans the period from ~~2015~~2014 to 2023 and includes measurements taken at a depth of 10 cm (deeper
239 soil layers were not analysed; Pütz et al., 2016).

240 *2.1.2 Definition of Reference Site for Model Framework*

241 For model development, a single lysimeter moved from Dedelow to the Bad Lauchstädt lysimeter
242 station (see Fig. 3a and 3b) was selected as the training dataset. This lysimeter was chosen due to its
243 stable soil water content dynamics and minimal temporal drift in water retention properties over the
244 observation period (see Fig. 4a). This lysimeter served as the reference dataset for developing the
245 predictive model because it allows the definition of soil water content response function for the seasonal
246 climatic conditions. The 23 remaining lysimeters at the Bad Lauchstädt and Selhausen site were used
247 as independent test datasets (a contrasting example is shown in Fig. 4b) to evaluate model generalization
248 and detect potential shifts in soil hydraulic behaviour across sites and years.

Formatted: Not Superscript/ Subscript



249

250

251 **Figure 4** Soil water retention curves using data collected between 2015 and 2023 at 10 cm depth. Matric potential
 252 is plotted against volumetric water content, with data colour-coded by period: 2015–2016 (blue), 2017–2020
 253 (green), and 2021–2023 (red). (a) Training lysimeter (moved from Dedelow to Bad Lauchstädt). (b) Test lysimeter
 254 (original soil from Selhausen in lysimeter station at Selhausen).

255 2.2 Data Preprocessing and Feature Engineering

256 All raw data were aggregated or resampled to a daily time step to support time-series analysis and
 257 modelling. Any misaligned or duplicated timestamps were corrected to ensure consistency.
 258 Measurements before the year 2015 were excluded from both sites to allow sensor settlement after
 259 installation.

260 2.2.1 Seasonal-Trend decomposition

261 ~~After cleaning and aligning the data, the climatic variables used as inputs in the modelling were selected.~~
262 ~~In addition to raw P and PET data, the daily climatic water balance (WB) was included as an explicit~~
263 ~~input. This variable reflects the net difference between P and PET, serving as a proxy for wetting or~~
264 ~~drying conditions. Positive values indicate potential moisture accumulation (e.g., during rainfall~~
265 ~~dominated periods), while negative values reflect high evaporative demand and drying conditions (e.g.,~~
266 ~~during hot, dry days). Including the WB helps the model to distinguish humid periods from dry ones.~~
267 ~~By providing WB alongside P and PET, the model can learn both the individual and combined effects~~
268 ~~of P and evaporative demand on soil water content dynamics (Brocca et al., 2010; Uher et al., 2018).~~
269 ~~For example, it can infer that 10 mm of P during a high PET summer day (low positive or negative WB)~~
270 ~~is less likely to increase soil water content than the same P on a cool, low-PET Day (high positive WB).~~

271 To provide the model with structured representations of climate variability, each climatic time series
272 was decomposed into additive components using STL based on LOESS with LOESS as acronym for
273 ‘Locally Estimated Scatterplot Smoothing’ (Cleveland et al., 1990). STL is a non-parametric method
274 that separates a time series into three interpretable parts: a seasonal component representing repeating
275 seasonal patterns (such as wetting and drying cycles), a trend component capturing gradual long-term
276 changes (such as climate shifts), and a residual component containing short-term irregularities and high-
277 frequency noise (Cleveland et al., 1990). This decomposition was applied independently to the P, PET,
278 and WB time series. Only the seasonal and trend components were retained as input features, as they
279 contain meaningful patterns relevant to soil water content dynamics. The residual component, which
280 lacks systematic structure, was excluded from further analysis. STL was configured with a cycle length
281 of 180 days, representing the semi-annual wet–dry phases at the study sites. A LOESS smoother with
282 a 90-day window was then applied to the de-seasonalized series to extract the trend component. This
283 configuration was chosen to capture gradual, long-term changes in the climatic variables while reducing
284 short-term fluctuations. Note, that near the ends of the time series the absence of future values causes
285 the smoothing window to become asymmetric. As a result, the estimated trend becomes more sensitive
286 to recent variability. This limitation does not affect the outcome of the analysis, as both the input
287 features and the target variable (water content) are equally influenced by it. Each of the extracted

288 seasonal and trend components from P, PET, and WB was included as input to the neural network
289 alongside the original raw values. This allowed the model to learn structured seasonal behaviour—such
290 as distinguishing the rising phase of spring wetting up of the soil profile from the declining phase of a
291 summer dry-down—and to account for long-term shifts, such as gradual drying or changes in mean
292 climate conditions.

293 2.2.2 Wetness classification

294 In addition to the continuous climate-related features, a categorical input was included to describe the
295 soil's moisture condition as either 'dry', 'moderate', or 'wet'. These categories were defined using the
296 soil water content time series from the training site, with thresholds based on quantiles of the full
297 distribution. Specifically, values below the 30th percentile were labelled as 'dry', between the 30th and
298 70th percentiles as 'moderate', and above the 70th percentile as 'wet'. These categories were then
299 encoded numerically prior to modelling, using values of 30 for 'dry', 20 for 'moderate', and 1 for 'wet'.

300 This encoding allowed the categorical feature to be treated as an ordinal variable and integrated into the
301 neural network input layer alongside the other features. The thresholds were selected to provide clear
302 regime separation while ensuring sufficient observations per class for robust model training.

303 There are two reasons to include this feature. Firstly, the soil's current moisture condition can strongly
304 influence its response to P and PET (Western & Grayson, 1998). For example, under dry conditions,
305 more water can be absorbed by the soil due to its high storage capacity. In contrast, when soils are
306 already wet or near saturation, infiltration capacity is reduced, and additional rainfall is more likely to
307 result in runoff (Tromp-van Meerveld & McDonnell, 2006; Zehe & Blöschl, 2004). The second reason
308 is the motivation to use remote sensing data in similar follow up studies, which are not yet accurate
309 enough for modelling purposes but allow a general classification of the wetness status. Because (i)
310 corresponding information on soil matric potential cannot be deduced at larger scale from remote
311 sensing data and (ii) hysteresis in the soil water retention curve may lead to ambiguous thresholds, we
312 focus here on soil water content measurements.

313 Another choice for the model framework that must be discussed is the choice of percentile thresholds.
314 From a soil hydrological point of view, it would make sense that the thresholds defining the three classes
315 ‘wet’, ‘moderate’ and ‘dry’ are chosen individually for each lysimeter (a wet clay soil may have very
316 different water content values than a sandy soil). However, from a methodological point of view, we
317 prefer to ensure that the model does not require a long time series to determine quantiles of soil water
318 content data and that the model can be run solely based on the training site’s distribution. Accordingly,
319 the same percentile thresholds, derived from the training site, were applied to label daily water content
320 values at the prediction sites. Note, that the application of the same percentile thresholds for all sites is
321 not relevant for the detection of changes in the soil water content response function. Very similar results
322 will be obtained for a site-specific percentile definition as shown in the supplementary material (section
323 S1). After constructing all the above features, each daily input to the model consisted of (i) raw climate
324 variables (P, PET, and WB), (ii) the STL-derived seasonal and trend components for each of those
325 variables (six variables), and (iii) the categorical moisture label. All ten features were aligned by date
326 to ensure consistency across inputs. This combination of raw values, decomposed temporal signals, and
327 qualitative soil condition provides the model with a detailed daily representation of both external
328 climatic forcing and internal system state.

329 2.3 Neural Network Architecture and Training

330 To model daily volumetric soil water contents, a feed-forward neural network was implemented. The
331 architecture consisted of three hidden layers: two dense layers with 12 neurons each using ReLU
332 activation functions (Rectified Linear Unit), followed by a batch normalization layer, and a third dense
333 layer with 6 neurons. ReLU was chosen for its ability to introduce non-linearity while maintaining
334 computational efficiency and avoiding vanishing gradient problems during training (Lu et al., 2020;
335 Montesinos López et al., 2022). Batch normalization was applied to stabilize learning by reducing
336 internal covariate shift, which improves convergence speed and training stability (Montesinos López et
337 al., 2022). The output layer consisted of a single neuron with a linear activation function, which is
338 standard for continuous regression tasks such as predicting soil water content.

339 The network was trained using input features derived from daily observations at the reference lysimeter
340 at the Bad Lauchstädt site, covering the period 2015–2023. Prior to training, all continuous input
341 features were standardized to have a mean of zero and a standard deviation of one using z-score
342 normalization. The standardization parameters (mean and standard deviation) were computed solely
343 from the training dataset and applied unchanged to the validation [and test](#) sets at the training site, as
344 well as to the prediction sites, ensuring consistency across all data splits. The target variable, volumetric
345 soil water content, was preserved in its original physical units ($\text{m}^3 \text{m}^{-3}$), allowing for direct interpretation
346 of the model outputs and associated errors in hydrologically meaningful terms. The model was compiled
347 with the Adam optimizer, which adaptively adjusts learning rates and is widely used for its
348 computational efficiency and stable convergence- ([Kingma and Ba, 2015](#)). Mean squared error (MSE)
349 was used as the loss function due to its sensitivity to large deviations, making it suitable for continuous
350 regression tasks. To monitor generalization, 30% of the data was withheld as a validation set and
351 excluded from updating the weights between the nodes during training. The training procedure was
352 initially set to proceed for a maximum of 1000 epochs. To prevent overfitting, an early stopping
353 criterion was implemented based on validation loss. Specifically, training was terminated if no
354 improvement in validation performance was observed over a predefined number of consecutive epochs
355 (patience threshold). The model parameters from the epoch exhibiting the lowest validation loss were
356 retained for final evaluation.

357 2.4 Testing the Neural Network

358 After training, the model was applied to the remaining 23 lysimeters across both Selhausen and Bad
359 Lauchstädt, none of which were included in the training phase. All test inputs were processed using the
360 same structure and normalization parameters derived from the training data. As outlined in Section 2.1,
361 the experimental setup includes four soil types, each installed with three replicates at both sites (see Fig.
362 3). While the lysimeters at the Bad Lauchstädt lysimeter station share the same climatic setting as the
363 training site, the lysimeters at Selhausen represent a more humid region. Accordingly, the raw data and
364 seasonal trend data of the Selhausen climate were used as input for the prediction of soil water content
365 in lysimeters located at Selhausen. This configuration allows to evaluate (i) whether the soil water

366 content response function determined for the training remains valid for different climates and soil types,
367 and (ii) to detect potential temporal ~~or structural~~ changes in soil hydraulic behaviour. The evaluation
368 and classification procedures are described in the following two subsections.

369 2.5 Detection of Change in Soil ~~Water Content~~water content Response Function 370 Based on Error Metrics

371 As explained in the introduction, we use error metrics to detect changes in the soil water content
372 response function. While we use the Nash-Sutcliffe ~~Efficiency~~efficiency (NSE, see eq. 5) as a general
373 descriptor of model error, we investigate temporal changes in model performance based on the Mean
374 Bias (MB) that was calculated on an annual basis from 2015 to 2023. This year-by-year assessment
375 does not rely on predefined change points and enables the detection of gradual or abrupt shifts in model
376 performance directly from the data. MB measures the average signed difference between predicted and
377 observed values, providing an estimate of systematic overestimation or underestimation over time
378 (Moriassi et al., 2007; Liu et al., 2011) and is defined as:

$$379 \quad MB = \frac{1}{N} \sum_{i=1}^N (\hat{\theta}_i - \theta_i) \quad (1)$$

380 where $\hat{\theta}_i$ is the predicted volumetric water content at day i , θ_i is the corresponding observation and N
381 defines the number of available observations–prediction pairs. Although, the calculation uses daily
382 values, MB is aggregated over yearly intervals to produce a single value per year, capturing annual
383 patterns in prediction bias. Volumetric water contents ($\text{m}^3 \text{m}^{-3}$) were multiplied by 100 prior to
384 calculation, and MB is therefore reported in percentage (%). Positive MB values indicate systematic
385 overestimation by the model, while negative values reflect underestimation. The annual assessment of
386 MB allowed us to evaluate whether the soil water content response function remains consistent ~~across~~
387 ~~time or shows temporal dynamics.~~over time or shows temporal dynamics. Deviations between
388 predicted and observed water content can differ in sign across moisture conditions and event types, such
389 that opposite errors may partially cancel when averaged over a full year. Therefore, mean bias is
390 interpreted as an indicator of long-term temporal drift in model–observation differences, while soil
391 water retention curves are used here (see next section) to verify the physical consistency and direction

392 of detected changes; in cases where retention measurements are not available, robustness of bias trends
393 can alternatively be assessed by repeating the analysis using different temporal aggregation periods.

394 To classify the soil water content dynamics with respect to the resilience after the extreme summer
395 2018, we check if the deviation of the predictions based on a stable response function (developed with
396 the training data) changes over the years. When the deviation in the first year (2015; i.e., before the
397 drought) is different from the deviation in the year 2023, we consider that the soil water content response
398 function has changed (it is still possible that the response function may recover in the future) and the
399 soil water content dynamics is classified accordingly as ‘changed’. When the deviations at beginning
400 and end are similar, but there was a period between 2018 and 2022 with a different deviation level, we
401 conclude that the soil water content response function changed reversibly over time but recovered
402 within the observation window and the lysimeter is classified as ‘resilient’. Note that in resilience-
403 related literature, the system response to disturbance is often characterized by the time scale and rate of
404 recovery following perturbation (Scheffer et al., 2009). Here, we do not analyse the recovery rate in
405 more detail but based on the definition of the ‘resilient’ category the recovery rate must be smaller than
406 four years.

407 The soil water content response is considered as ‘stable’ when the deviations remain similar during the
408 entire observation period. (i.e., the same response function of soil moisture dynamics to climatic
409 condition can be used). As threshold we chose 1.52%, that equals the 3-fold of the standard deviation
410 of the nine yearly MB values computed for the training site. The classification of the time series was
411 thus expressed formally as:

412 ‘changed’: $|MB_{2023} - MB_{2015}| > 1.52\%$ (2)

413 ‘resilient’: $|MB_{2023} - MB_{2015}| \leq 1.52\% \wedge |MB_{20xx} - MB_{2015}| > 1.52\%$ (3)

414 ‘stable’: $|MB_{2023} - MB_{2015}| \leq 1.52\% \wedge |MB_{20xx} - MB_{2015}| \leq 1.52\%$ (4)

415 with the logical operator \wedge and the mean bias of a specific year with MB_{20xx} , that shows the largest
416 difference $|MB_{\text{year}} - MB_{2015}|$ for the time period between 2018 and 2022 (starting with dry year 2018).

Formatted: Font: (Intl) Cambria Math

417 As general information on the different response function, we calculated the [Nash–Sutcliffe efficiency](#)
418 [\(NSE\)](#) coefficient (Moriassi et al., 2007; Nash & Sutcliffe, 1970). The NSE is a standard metric for
419 hydrological model skill, with NSE = 1 indicating perfect agreement and NSE ≤ 0 stating that the model
420 predictions are no better than using the mean of the observations. Mathematically, it is defined as:

$$421 \quad NSE = 1 - \frac{\sum_{i=1}^N (\theta_i - \hat{\theta}_i)^2}{\sum_{i=1}^N (\theta_i - \bar{\theta})^2} \quad (5)$$

422 where $\hat{\theta}_i$ is the predicted volumetric water content at day i , θ_i is the corresponding observed value, $\bar{\theta}$ is
423 the mean observed volumetric water content over the evaluation period, and N denotes the total number
424 of valid data points used in the calculation. Following Moriassi et al. (2015), model performance was
425 classified as very good for NSE > 0.80, good for 0.70 < NSE ≤ 0.80, satisfactory for 0.50 < NSE ≤ 0.70,
426 and unsatisfactory for NSE ≤ 0.50. ~~Lower NSE values were interpreted as indicators of deviations from~~
427 ~~the soil hydraulic behaviour represented in the training data, potentially due to differences in soil~~
428 ~~properties or climate induced structural changes.~~

429 ~~In this study, NSE is used to summarize the overall agreement between simulated and observed soil~~
430 ~~water dynamics, whereas the identification and classification of temporal changes in the soil water~~
431 ~~content response function rely exclusively on the annual evolution of mean bias. Lower NSE values~~
432 ~~were interpreted as reduced dynamic agreement between the tested lysimeter and the reference soil–~~
433 ~~climate response used for training, without implying a specific mechanism of change.~~

434 2.6 Interpretation of Change in Response Function in Soil Physical Terms

435 The dynamics of MB (see above) was also used to assess changes in soil water retention curves
436 (SWRCs), which were plotted for each test lysimeter on a yearly basis. As stated in eq. (1), a positive
437 MB value corresponds to measured [water contents](#) values that are smaller than the predictions. Because
438 the predictions are based on the model trained for a specific lysimeter, we expect for a positive MB that
439 the water content for the same environmental conditions (as manifested in the matric potential) is
440 smaller in the test lysimeter compared to the lysimeter used for training (SWRC is shifted to the left).
441 Analogously, for a consistently negative MB we expect that the test site retained more water at a given
442 matric potential than the training site and the SWRC is shifted to the right. For a ‘resilient’ soil, the soil

443 water retention curve will be shifted over time and will shift back close to the original position at the
444 end of the observation period. Finally, for a soil with ‘changed’ response function, the water retention
445 curve is drifting over time as well but without returning to its original position. In some cases, the
446 temporal evolution of MB may not exactly follow the apparent shift of the SWRC, as additional vertical
447 or slope changes could occur due to variations in porosity or pore-size distribution. These effects cannot
448 be identified within the current framework but may contribute to deviations between MB dynamics and
449 the apparent SWRC shift. [To further support the SWRC-based interpretation, a quantitative analysis of](#)
450 [soil water retention curve evolution based on the concept of integral mean water content is provided in](#)
451 [the Supplementary Material.](#)

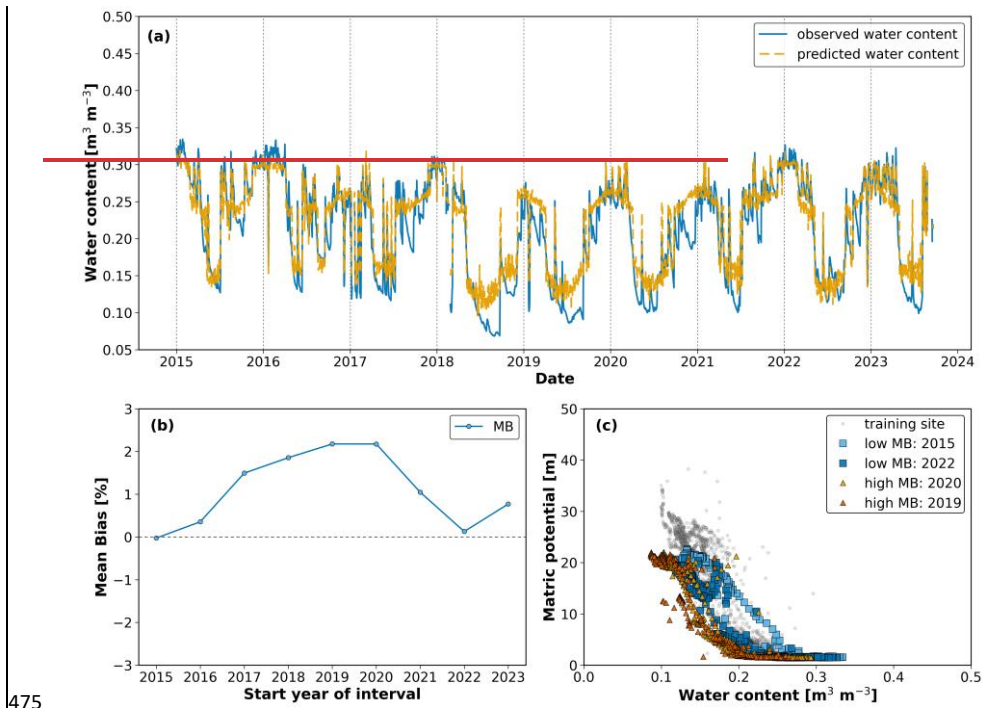
452 3. Results

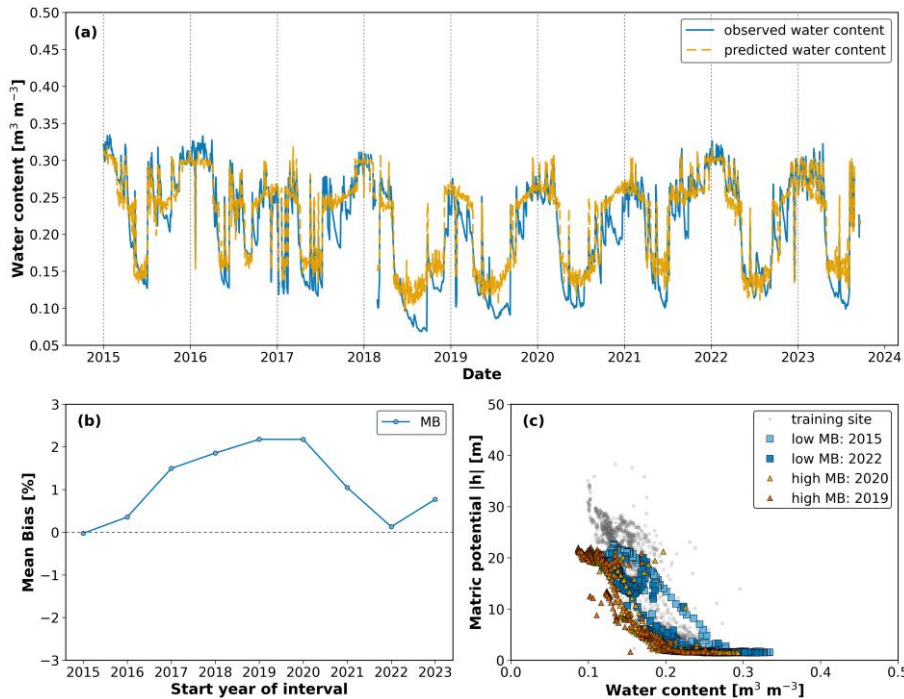
453 Following the methodological framework described in Section 2.3-2.6, we present the results of model
454 predictions across the test lysimeters to assess the resilience of the soil water content response function
455 for the different lysimeters. We organize the section in four subsections according to the four different
456 origins of the soil in the lysimeters (see Fig.3b) to discuss effects of soil origin and climatic conditions
457 on the response function. In the last subsection (3.5) the results are summarized to allow direct
458 comparison of all 24 lysimeters. Note, that all model results presented below are based on the soil water
459 content classification (‘wet’, ‘moderate’, ‘dry’) as deduced from the lysimeter used for model training.
460 The corresponding figures using specific classification for each lysimeter are shown in supplementary
461 information Fig. S4-S7.

462 3.1 Lysimeters with ~~Same Soils~~ [same soil as Used](#) ~~used~~ [in Model Training](#) ~~model~~ 463 [training \(Dedelow ~~Soils~~soils\)](#)

464 The neural network was trained to capture the soil water content response function of one lysimeter
465 with sandy loam topsoil (Luvisol) extracted from Dedelow and translocated to the dry climatic region
466 in Bad Lauchstädt (see Fig. S1 in supplementary material). The NSE of the training and validation of
467 that specific lysimeter was very high with 0.91 indicating good model performance. The application of
468 this response function to the other two lysimeters from Dedelow that were translocated to Bad

469 Lauchstädt ~~resulted~~ in relatively high NSE values (0.79 and 0.84). ~~However,~~ but the response in
 470 summer 2018 with lower soil water ~~contents observed during the summer of 2018 were~~ content was not
 471 ~~adequately~~ captured properly as shown in Fig. 5a. More specifically, the time series show that
 472 predictions and observations matched closely in 2015, while after the dry summer of 2018 the model
 473 systematically overestimated water content in 2019 and 2020, before the agreement improved again
 474 towards the end of the period.





476
 477 **Figure 5** Analysis of soil water content dynamics (2015–2023) for a Dedelow-origin lysimeter tested at Bad
 478 Lauchstädt. Panel (a) shows the time series of observed (blue) and predicted (orange) water content, with close
 479 agreement in 2015, clear overestimation in 2019–2020 (predictions above observations), and improved
 480 agreement again towards the end of the period. Panel (b) presents the temporal evolution of mean bias (MB),
 481 remaining near zero until 2017, increasing to about 2–3% in 2019–2020, and decreasing again to approximately
 482 zero in 2022. Such soil water content response was classified as ‘resilient’. Panel (c) displays soil water retention
 483 curves from the training site (grey) and from selected years representing different MB conditions, with low-MB
 484 years (2015, 2022) and high-MB years (2019, 2020). The curves are close to the training site in 2015, show a
 485 shift to lower water contents in 2019–2020, and in 2022 return to the training site data.

486 These changes are reflected in the MB development (Fig. 5b), with values increasing from near zero in
 487 2015 to about 2–3% in 2019–2020 and then decreasing again towards 2022. The retention curves
 488 confirm this interpretation (Fig. 5c). The year with low MB (2015) produced a SWRC close to the
 489 measured curve of the training site, the years with high MB (2019–2020) were shifted to lower water
 490 contents, and the later year with reduced MB (2022) returned to the measured SWRC of the training
 491 site. Taken together, the time series, MB trend, and SWRCs show that the soil response was disturbed
 492 after 2018 but later recovered, defining this lysimeter as ‘resilient’. The same finding holds for the

493 simulations for the lysimeters translocated to Selhausen (less dry climate) with high NSE between 0.80–
494 0.82. This indicates, that for ~~this~~the coarse-textured soil included in this study (i) the effect of changing
495 climatic conditions was rather small (very good NSE classification for both sites), but (ii) that ~~also~~
496 these coarse-textured topsoils do not show identical response to the extreme year ~~but, as~~ each lysimeter
497 reacts slightly ~~different, indicating slightly different structural~~differently, which may indicate small
498 differences in hydraulic properties.

Formatted: Font: (Default) +Headings CS (Times New Roman)

499 3.2 Lysimeters with ~~Soils Adapted to Climatic Conditions Similar with Those of~~ 500 the Model Training Sites~~soils formed under the same climate as the one used in~~ 501 model training (Bad Lauchstädt soil)

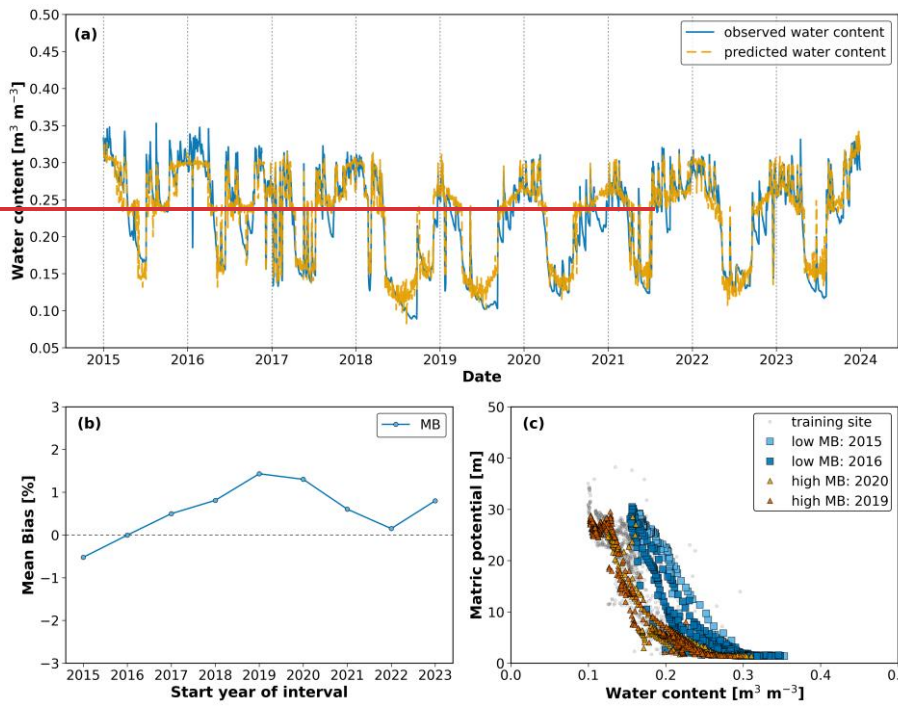
502 The lysimeters filled with soil from Bad Lauchstädt (Chernozem) ~~represent soils adapted to~~were formed
503 under the climatic conditions ~~under which~~used for the fitting of the response function ~~was calibrated.~~

504 In case of dominant effect of climate on the soil water content response function, we could expect
505 similar results as for the training lysimeter. For the soil remaining at the original site (Bad Lauchstädt),
506 the model performance was very good (0.88–0.89). As shown for an example in Fig. 6a, the fit between
507 observed and predicted water content was consistently close, with a tendency to slightly underestimate
508 in the early years and to mildly overestimate after 2018, particularly in 2019–2020, before the agreement
509 improved again in later years. This is also manifested in the MB values that increased from slightly
510 negative values in 2015 to about +1.5% in 2019, before decreasing again towards zero (Fig. 6b). The
511 plotted SWRCs support this interpretation (Fig. 6c), with low MB years (2015 and 2016) showing a
512 slight shift to higher water contents relative to the measured SWRC of the training site, and high-MB
513 years (2019 and 2020) displaying a modest shift to lower water contents. Accordingly, the soil water
514 content dynamics was classified as ‘resilient’.

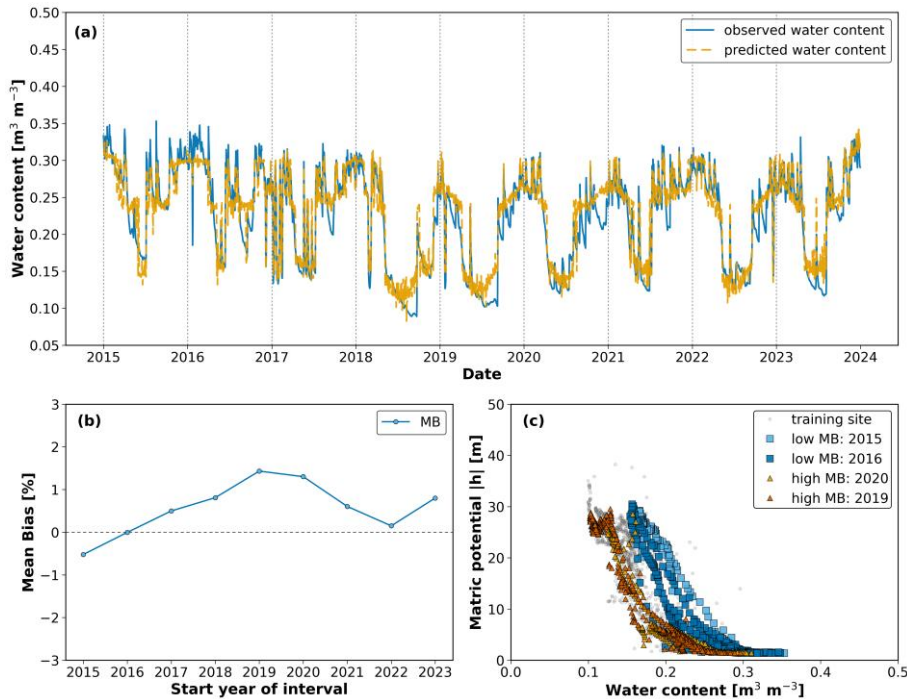
515 For the lysimeters transported from Bad Lauchstädt to Selhausen, the performance was more variable
516 (NSE ranging from 0.50 to 0.84) corresponding to satisfactory to very good classifications, reflecting
517 the stronger effect of the wetter climate. None of the three lysimeters ~~who~~that stayed in Bad Lauchstädt
518 were classified as ‘changed’ but two out of three showed a systematic shift and were classified as
519 ‘changed’ when translocated to Selhausen (see Table 1). In short, ~~these~~these examples show that the

520 Bad Lauchstädt soil remained resilient under ~~unchanged climate~~ its original climatic conditions at Bad

521 Lauchstädt but changed ~~under when exposed to the wetter climate~~ climatic conditions at Selhausen.



522

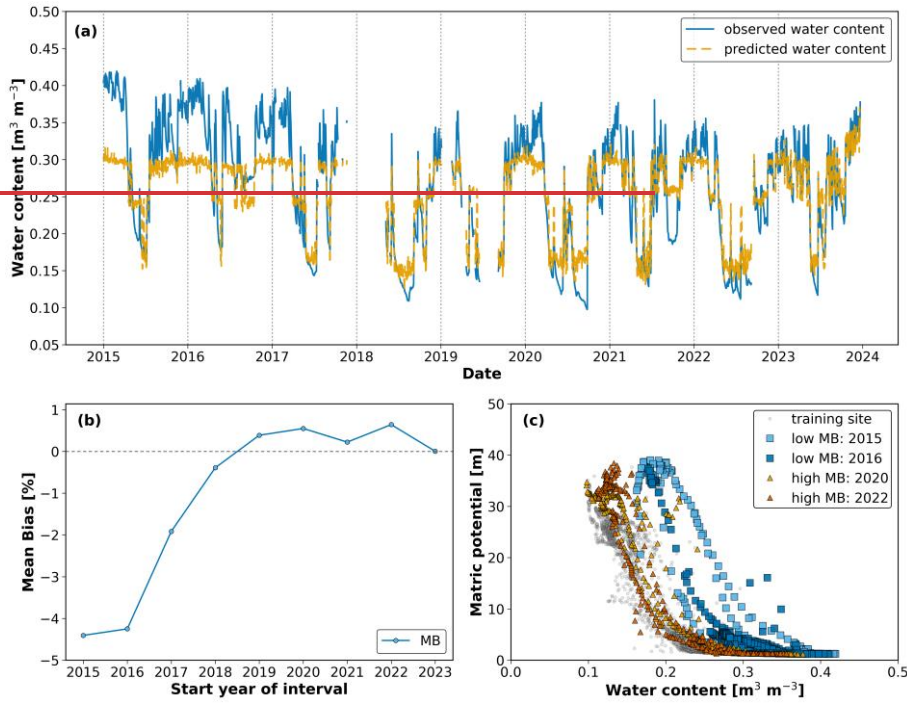


523
 524 **Figure 6** Analysis of soil water content dynamics (2015–2023) for a Bad Lauchstädt-origin soil lysimeter tested
 525 at Bad Lauchstädt. (a) Comparison of measured (blue) and simulated (orange) daily water content values,
 526 showing high agreement in the early years and temporary overestimation in 2019–2020. (b) Mean Bias (MB)
 527 started slightly negative in 2015, increased to about +1.5 % in 2019, and then decreased again towards 2022. (c)
 528 Soil water retention curves (SWRCs) from the training site (grey) and from the same replicate for selected years
 529 with low MB (2015, 2016) and high MB (2019, 2020) show close agreement in the early years and a shift to lower
 530 water contents in 2019–2020.

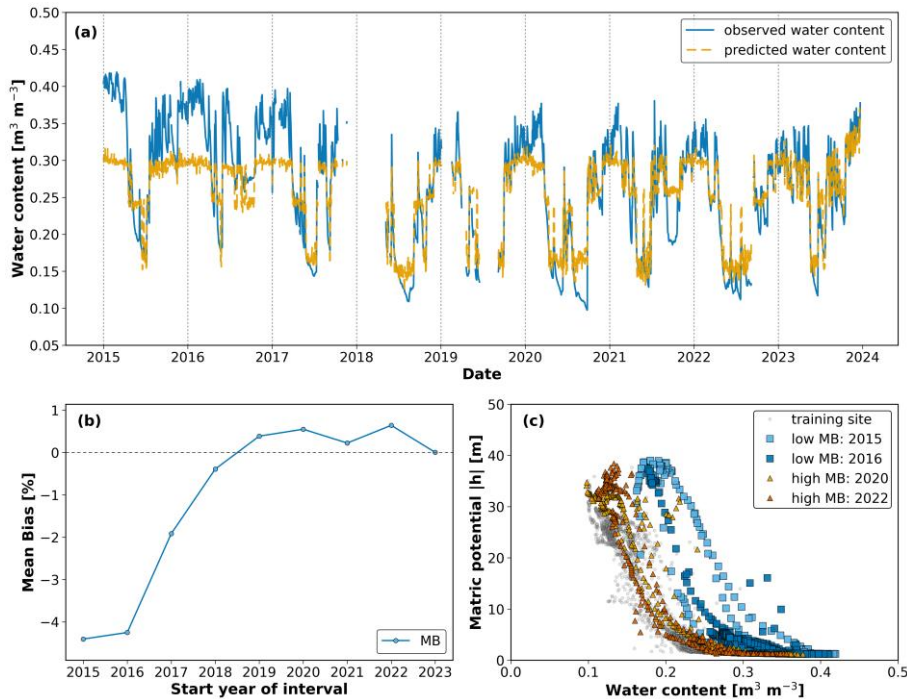
531 3.3 Lysimeters with ~~Soils Adapted to Climatic Conditions comparable with Those~~
 532 ~~of soils formed under similar climate as the Model Training Site~~ used in
 533 ~~model training~~ (Sauerbach soil)

534 The findings are similar for the silt loam (Cambisol) from Sauerbach, ~~representing soils adapted to that~~
 535 ~~was formed under similar~~ climatic ~~conditions comparable to condition as~~ those in Bad Lauchstädt. As
 536 in case of the soil from Bad Lauchstädt, soils from Sauerbach show higher NSE values when
 537 translocated to Bad Lauchstädt (0.81–0.88, very good) compared to those transferred to the wetter
 538 climate in Selhausen (0.74–0.79, good). This reflects, that the soil water content response function in
 539 the drier climate is not the same as in the wetter climate. In one illustrative case, the observed water

540 content initially showed wetter dynamics than predicted, but gradually converged toward the model
541 predictions by 2023, indicating a possible ~~structural~~ adjustment in soil hydraulic response over time
542 (Fig. 7a).



543



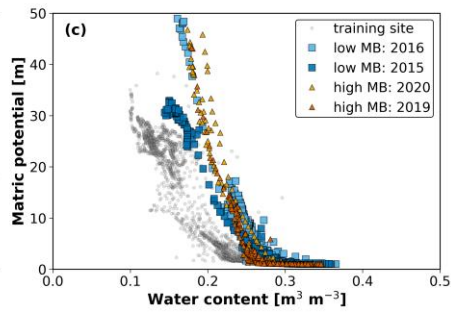
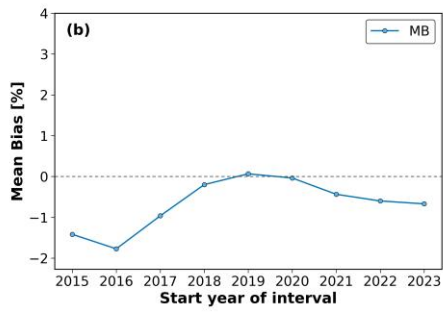
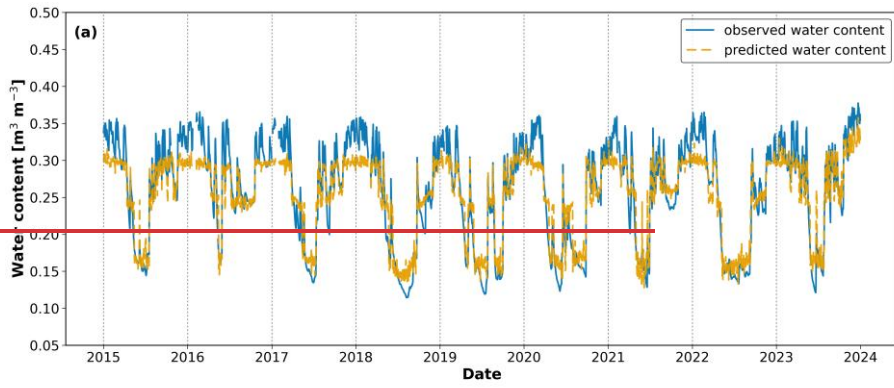
544
 545 **Figure 7** Analysis of soil water content dynamics (2015–2023) for Sauerbach-origin lysimeter relocated to
 546 Selhausen (a) Comparison of observed and predicted daily volumetric water content ($NSE = 0.74$). After initial
 547 underestimation by the model, the observed and predicted values gradually converged, indicating a possible
 548 *structural-adjustment in soil hydraulic behaviour over time*. (b) Temporal evolution of the mean bias (MB), which
 549 increased from about -5% in 2015 to values close to zero by 2019–2023, consistent with the improved match
 550 between observed and predicted values shown in panel (a). (c) Soil water retention curves (SWRCs) from the
 551 training site (grey) and from selected years with low MB (2015, 2016) and high MB (2020, 2022) illustrate the
 552 same trend, with early years showing higher water contents at a given matric potential and later years shifting
 553 towards to the training curve.

554 This development is also evident in the MB values (Fig. 7b), which started strongly negative (-5%) in
 555 2015–2016 and steadily increased toward values close to zero by 2023, indicating a progressive
 556 reduction of underestimation. The corresponding SWRCs (Fig. 7c) confirm this trend, with curves from
 557 early years (2015, 2016) showing higher water contents at a given matric potential compared to the
 558 measured SWRC of the training site and later years (2021, 2023) shifting closer to the reference,
 559 suggesting a gradual adjustment of hydraulic behaviour. In the case of soils from Sauerbach, there was
 560 a difference in quantification of resilience with respect to the classification of the soil water content

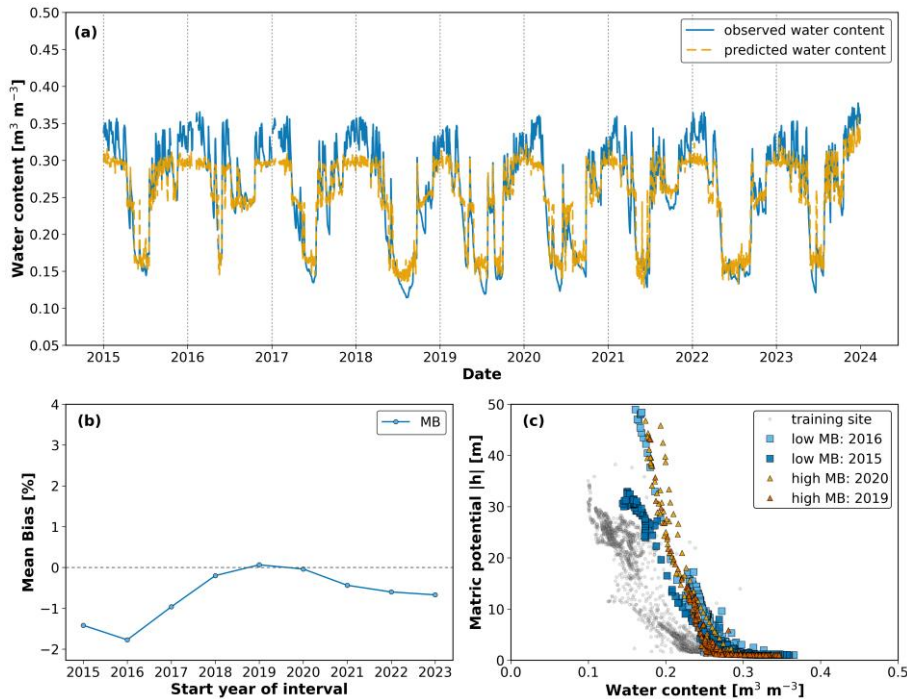
561 used as input variable: with the classification based on the training lysimeter (with sandy loam in the
562 topsoil), the soil water content dynamics was classified as ‘changed’ for all six lysimeters. But using
563 the classification based on the soil water content statistics obtained for each lysimeter individually (see
564 Fig. S6), the large water contents at the beginning were captured and only one lysimeter out of three
565 was classified ‘changed’. Independent of the water content classification, all lysimeters translocated to
566 Selhausen were classified as ‘changed’, exhibiting the strongest response to relocation of all soils.

567 3.4 Lysimeters with ~~Soils Adapted to Climatic Conditions Different from Those of~~ 568 ~~the Model Training Sites~~soils formed under different climate compared to the 569 ~~one used in model training~~ (Selhausen)

570 At last, we discuss the Selhausen silt loam (Luvisol), ~~representing soils adapted to climate~~which was
571 ~~formed under weather~~ conditions that were not ~~included~~used in the ~~training of the~~ neural network
572 ~~training~~. The model performance was better for the replicates translocated to the drier Bad Lauchstädt
573 climate (NSE = 0.86–0.92, very good), compared to slightly lower performance at their site of origin
574 under humid Atlantic conditions (0.76–0.86, good to very good). The classification with respect to
575 resilience helps to explain this, since Selhausen soils at their origin were mainly assigned to ‘stable’ or
576 ‘resilient’ categories (see Table I), while the same soils translocated to Bad Lauchstädt showed a more
577 variable pattern. This indicates, that the lower NSE at Selhausen does not represent a misfit of the model
578 but reflects that the soils follow their own stable soil water content response function. One replicate at
579 Selhausen (NSE = 0.85) reproduced the seasonal dynamics well, although differences between observed
580 and predicted values remained visible in the wet season across several years (Fig. 8a). The MB shifted
581 from negative values in the first years toward zero after 2019. Note, that an MB value of 0 does not
582 mean that deviations disappeared, but that errors in wetter and drier phases compensated each other
583 (Fig. 8b). The SWRCs were generally close to the training reference, but in later years small deviations
584 appeared mainly at the saturated end (Fig. 8c). Overall, these changes remained below the assumed
585 threshold, supporting a classification of the soil water content dynamics as ‘stable’.



586



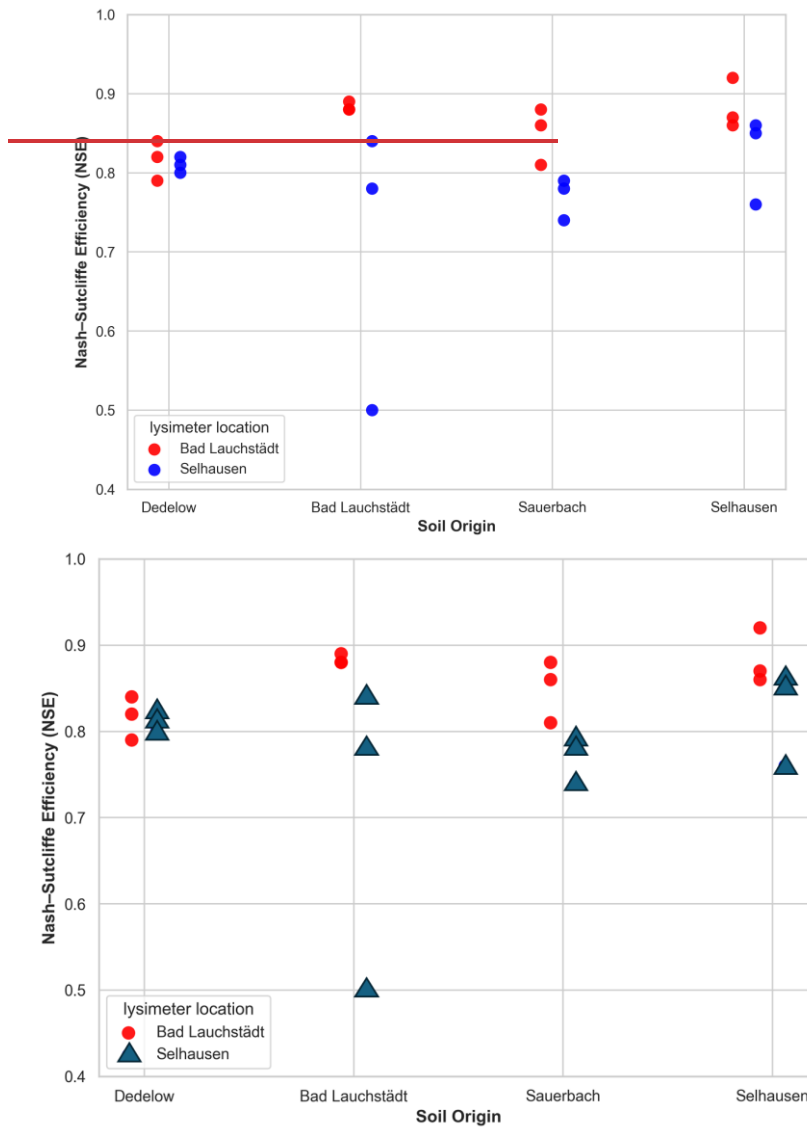
587 **Figure 8** Soil water content dynamics (2015–2023) for a Selhausen-origin lysimeter tested at Selhausen. (a)
 588 Observed (blue) and predicted (orange) water content show fair agreement, with underestimation of water
 589 contents in the wet season. (b) Mean Bias (MB) fluctuated from negative values in the early years to values close
 590 to zero after 2019, but these variations remained below the threshold for change. (c) Soil water retention curves
 591 (SWRCs) from the training site (grey) and from selected years with low MB (2015, 2016) and higher MB (2019,
 592 2020) reflect these minor variations, with the 2019 curve showing the strongest deviation yet remaining close to
 593 the training reference, consistent with the stable classification. The apparent cutoff at the wet end in (a) arises
 594 from the use of absolute rather than normalized values during training, as discussed in the Supplementary
 595 Material (Text S1).
 596

597 **3.5 Comparison of All Lysimeters all lysimeters**

598 The comparison of the soil water content dynamics of all lysimeters indicate, that **contrasting** climatic
 599 **shifts** conditions between sites, **—** particularly between the continental Bad Lauchstädt and Atlantic-
 600 influenced Selhausen **—** can significantly alter the hydraulic response of the soil, even when texture
 601 remains constant. In general, prediction performance at Selhausen was lower, likely because the model
 602 was trained under the drier climate of Bad Lauchstädt, and therefore, failed to fully capture the soil-
 603 water interactions emerging under wetter conditions (Fig. 9). The broader NSE range observed at

Formatted: Font: Arial, Font color: Custom Color(RGB(10,10,10)), Pattern: Clear (White)

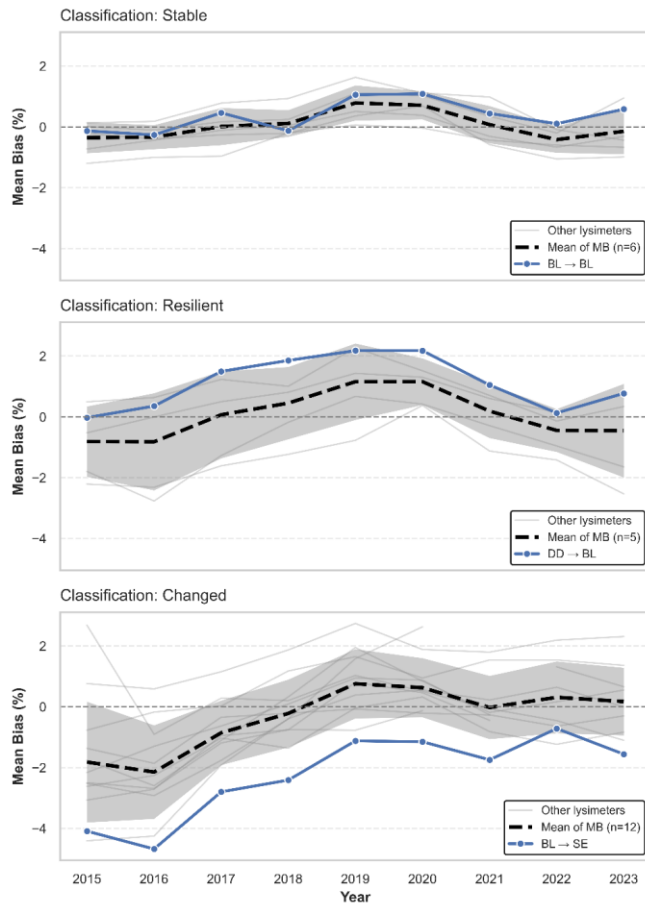
604 Selhausen location further suggests increased ~~structural~~ variability in hydraulic response among
 605 replicates.



607
 608 **Figure 9** Spread of Nash-Sutcliffe ~~Efficiency~~ efficiency (NSE) values across different soil origins and test
 609 locations. Each symbol represents one lysimeter from a given origin (x-axis) evaluated at Bad Lauchstädt or
 610 Selhausen (indicated by colour). The results highlight the influence of climate-soil interactions on model
 611 performance. Notably, Bad Lauchstädt-origin soils exhibited strong performance at their origin but a wider and

612 lower range when tested at Selhausen, ~~reflecting~~ ~~indicating~~ increased ~~structural~~ variability ~~or~~ ~~climate-induced~~ in
613 ~~soil hydraulic behaviour and~~ divergence in ~~hydraulic~~ soil-climate response.

614 With respect to resilience of the soil water content response function, we show the temporal evolution
615 of the mean bias for all lysimeters in Fig. 10 and summarize the results in Table 1. In Table 1 we add
616 the general classification type ('stable', 'resilient' and 'changed') and calculate the average of 3
617 lysimeters (same material and same location) for the drift in mean bias value between the year 2015
618 and 2023 and the maximum deviation from year 2015 for the years between 2018 and 2022. The table
619 shows that deviations from a 'stable' or 'resilient' response function mainly occur when soils from
620 Dedelow, Bad Lauchstädt, and Sauerbach were translocated to Selhausen. Only in case of the soil from
621 Selhausen, the response function remains 'stable'. It seems, that the soil material 'trained over decades'
622 to the wetter climate in Selhausen adapts better to the extreme summer 2018.



623
 624 **Figure 10** Temporal evolution of Mean Bias (MB) for three representative lysimeter replicates, each classified
 625 into one of three structural soil hydraulic response categories: (a) 'stable', (b) 'resilient', and (c) 'changed'.
 626 Thick dashed lines indicate the mean of the MB trend across all lysimeters within each classification group, with
 627 sample size (n) specified in the legend. Shaded areas represent ± 1 standard deviation. Thin grey lines show
 628 individual MB trajectories of the remaining lysimeters in each group. Highlighted blue lines depict selected
 629 replicates originating from and/or tested at distinct sites: (a) BL \rightarrow BL (soil material from Bad Lauchstädt tested
 630 at its origin), (b) DD \rightarrow BL (soil material from Dedelow tested at Bad Lauchstädt), and (c) BL \rightarrow SE (soil material
 631 from Bad Lauchstädt tested at Selhausen). These examples illustrate contrasting temporal patterns in
 632 structural hydraulic response, ranging from sustained stability to progressive divergence from the trained site
 633 dynamics.

634 **Table 1:** Resilience of soil water content response function for the four soil materials translocated to Bad
 635 Lauchstädt and Selhausen. The 'type' describes the class of response function of the individual lysimeters (S for
 636 'stable', R for 'resilient' and C for 'changed'). The 'drift' is the average value $|\text{MB}_{2023} - \text{MB}_{2015}|$ of the three

637 lysimeters with the difference in Mean Bias (MB) between years 2023 and 2015. The ‘amplitude’ is the maximum
 638 difference of the Mean Bias between the first year (2015) and the years between 2018 and 2022 (denoted as year
 639 20xx).

	Located at Bad Lauchstädt			Located at Selhausen		
	Type	Drift	Amplitude	Type	Drift	Amplitude
Dedelow	S,R,C	1.09	1.76	R,C,C	1.72	2.11
Bad Lauchstädt	S,S,R	0.94	1.36	R,C,C	2.15	2.99
Sauerbach	C,C,C	2.17	3.73	C,C,C	3.38	4.24
Selhausen	S,R,C	0.96	2.24	S,S,R	0.47	1.78

640

641 4. Discussion

642 The results presented in Section 3 demonstrate that the model can reproduce soil water content dynamics
 643 reliably under stable conditions (as indicated by high NSE-values), but it exhibits limitations when soils
 644 undergo **structural** **persistent** changes **in hydraulic behaviour** or are exposed to a different climate.
 645 Several soils showed a shift in the wet range, indicating that differences in soil water content response
 646 cannot be explained by texture alone but reflect the combined effects of climatic conditions and
 647 structural evolution. Based on these findings, the following discussion evaluates how assumptions of
 648 static hydraulic behaviour and response function affect model performance, examines the role of NSE
 649 and MB in identifying evolving system dynamics, and reflects on the broader implications for long-
 650 term modelling and soil water content monitoring.

651 4.1 Soil–Climate Interactions as Drivers of Hydraulic Response Function

652 The predictive success of data-driven models depends not only on the physical properties of soils but
 653 also on the climatic context in which those properties developed and continue to function. The present
 654 study shows that soils exhibit the most consistent replicate behaviour when evaluated under climate
 655 conditions similar to those of their origin, where gradual climatic changes over time have allowed their
 656 structure to adjust naturally. When exposed to faster or contrasting climatic shifts, as in translocated
 657 settings, the soil response becomes less predictable and less stable. This can be shown using the table
 658 S1 in the supplementary material file, which lists the average trends (difference in MB between year
 659 2023 and 2015) and amplitudes (difference in MB between 2015 and the dry years) for three lysimeter

Formatted: Font color: Auto

Formatted: Font color: Auto

Formatted: Font color: Auto

Formatted: Font color: Auto

Formatted: Font color: Auto

Formatted: Font color: Auto

Formatted: Font color: Auto

Formatted: Font color: Auto

Formatted: Font color: Auto

Formatted: Font color: Auto

Formatted: Font color: Auto

Formatted: Font color: Auto

Formatted: Font color: Auto

Formatted: Font color: Auto

Formatted: Font color: Auto

Formatted: Font color: Auto

Formatted: Font color: Auto

Formatted: Font color: Auto

Formatted: Font color: Auto

Formatted: Font color: Auto

Formatted: Font color: Auto

Formatted: Font color: Auto

Formatted: Font color: Auto

Formatted: Font color: Auto

Formatted: Font color: Auto

660 replicates: only for the three lysimeters at the original locations Bad Lauchstädt or Selhausen), both
661 drift and amplitude were below the stability threshold of 1.52% and can be classified as ‘stable’ as group
662 of lysimeters.

663 This suggests that the ~~structure and~~ function of the soil system cannot be meaningfully decoupled from
664 its climatic history. Soils may develop pore arrangements, aggregation patterns, and, as a consequence,
665 moisture retention characteristics that reflect long-term adaptation to local hydrological regimes. When
666 these soils are translocated to environments with contrasting ~~P~~precipitation and atmospheric demand
667 (~~PET~~), their hydraulic response can shift in ways that are not captured by static texture-based estimates
668 of soil hydraulic properties. Alternative pore-scale processes, including slowly reversible swell–shrink
669 behaviour and non-equilibrium preferential flow, may also contribute to the observed shifts in apparent
670 SWRC behaviour. Recent large-scale analyses have demonstrated statistically significant impacts of
671 climatic factors on soil pore space organisation and laboratory-measured retention characteristics
672 (Hirmas et al., 2018; Klöffel et al., 2024), providing independent support for the plausibility of climate-
673 driven modification of soil hydraulic response.

674 Such context-dependent behaviour highlights the limitation of the common assumption that soils with
675 the same texture will show comparable retention across regions, an assumption often made in the
676 absence of better descriptors. ~~Experimental~~ While laboratory-measured SWRCs show strong and well-
677 established correlations with texture across climatic gradients, particularly in the dry range,
678 experimental evidence collected under natural field conditions ~~also~~ indicates that this simplified
679 description ~~is oversimplified~~ does not always hold (Hannes et al., 2016; Robinson et al., 2016; Aqel et
680 al., 2024). In our case, even soils with similar textural composition exhibited different levels of model
681 agreement depending on climate, highlighting that physical similarity (e.g. soil texture) does not
682 guarantee functional equivalence in retention. For example, Selhausen-origin soils achieved higher NSE
683 values when translocated to Bad Lauchstädt, likely because the model was trained under similar dry
684 climatic conditions. However, classification results showed, that these soils retained greater ~~structural~~
685 stability at their origin, suggesting that predictive success under familiar climatic forcing does not
686 necessarily imply hydraulic consistency. After the 2018 drought, the Selhausen soils translocated to
687 Bad Lauchstädt converged toward similar dynamics across replicates, with MB stabilizing close to zero,

688 indicating that their response functions adjusted consistently to the drier climate (see Fig. S2 in the
689 supplementary material). However, a clear carry-over effect was observed: soil water in the upper 10
690 cm was not fully replenished during the wet phase of autumn and winter 2019 and only reached
691 comparable, though slightly lower, values in winter 2020. ~~This persistent deficit points to a structural
692 legacy of the drought, where reduced pore connectivity and altered aggregation limited subsequent
693 rewetting.~~ A comparable multi-year legacy across the full soil column was reported in the TERENO-
694 SOILCan lysimeter network by Groh et al. (2020).

695 All mentioned points underscore the importance of including very broad range of climatic forcing in
696 the assessment of soil model transferability, as demonstrated by Groh et al. 2022. Our results also
697 suggest that future efforts to generalize hydrological models should consider training under a range of
698 climatic conditions to capture the full expression of soil–climate interactions, rather than relying on a
699 single static representation. From a process-based perspective, these findings reflect that climate does
700 not simply modulate soil water content inputs but actively shapes the retention and release behaviour
701 of the soil pore network ~~through structural evolution or breakdown by driving changes in soil hydraulic
702 response.~~ While management practices across sites were similar, minor differences in tillage and
703 fertilization cannot be completely excluded and may have influenced soil structure and water retention.

704 ~~In addition, monitoring of soil organic matter over time would be illustrative to link the change in the
705 response function and structure related soil hydraulic properties to biological processes. Another
706 mechanism that could result in structural changes is swelling and shrinking of the soils with
707 considerable clay amount (three soils with ~20% clay).~~ Nonetheless, the dominant control remains
708 climatic forcing, which makes this consideration particularly relevant for climate-change experiments:
709 models calibrated under past climatic conditions may not remain valid under the rapid climatic shifts
710 projected for the coming decades. Neglecting this evolving soil–climate feedback could lead to
711 substantial underestimation of future changes in soil hydraulic behaviour and associated ecosystem
712 responses.

713 4.2 High Predictive Performance Can Mask System Evolution

714 Although, several lysimeters achieved high predictive performance as expressed by high NSE values
715 (Fig. 9), systematic trends in MB over time suggest that the underlying retention behaviour and soil
716 water content response function may have shifted (Fig. 10 and Table 1). This was most apparent in
717 Dedelow soils translocated to Bad Lauchstädt, where the model maintained high NSE values, but the
718 MB increased across years (see Fig. S3). The corresponding shifts in the soil water retention curves
719 confirmed a gradual change in how the soil retained water, despite the model continuing to predict
720 moisture levels accurately.

721 This suggests that local ~~structural changes in hydraulic behaviour~~ can occur without immediate
722 deterioration in model fit. The predictive framework remained effective in capturing the general
723 moisture dynamics, but the relationship between matric potential and water content was no longer
724 consistent with that observed during training. These findings highlight that high model accuracy does
725 not guarantee stability in the hydraulic characteristic, particularly under changing environmental
726 conditions. Identifying such divergence early is critical for maintaining reliable predictions in long-term
727 monitoring.

728 4.3 Implications for Monitoring, Remote Sensing, and Soil Health

729 The classification outcomes across all lysimeters highlight the role of site memory and
730 ~~structural hydraulic~~ resilience in maintaining ~~hydraulic behaviour~~ soil water response under climatic
731 stress. Soils assessed at their origin were more frequently classified as ‘stable’ or ‘resilient’ (e.g.,
732 Selhausen at Selhausen), while those translocated to different locations were more likely to be classified
733 as ‘changed’ (e.g., Sauerbach at Bad Lauchstädt). ~~These~~ As was stated in the method section, this
734 classification as ‘changed’ is affected by the length of the observation window and does not allow
735 definitive decision between a persistent change to a new response function and a manifestation of a low
736 recovery rate. Independent of future development, these patterns indicate that soil ~~structure, once~~
737 ~~adapted to specific climate regimes,~~ hydraulic behaviour shaped by long-term climatic adaptation may
738 ~~lose its functional integrity~~ change when soils are exposed to new environmental conditions. The
739 presented methods allow ~~us to detect~~ detection of emerging ~~structural~~ shifts in soil hydraulic behaviour

740 that may be relevant for soil health assessment and could ~~be used as indicator for deteriorated~~ serve as
741 indicators of deteriorating soil health status. The presented methods allow us to detect emerging
742 hydrological shifts that may be relevant for soil functioning and could serve as indicators of potential
743 soil health deterioration.

744 This has direct implications for long-term monitoring and remote sensing. Our model framework ~~—~~
745 by avoiding reliance on matric potential data and instead using moisture state categories and
746 decomposed climatic features ~~—~~ is compatible with satellite-derived products. As remote sensing
747 missions increasingly provide continuous global soil water content estimates, the proposed framework
748 could be adapted for large-scale assessment of soil system stability. Furthermore, under scenarios of
749 future climate change, where shifts in precipitation patterns and evaporative demand are expected, data-
750 driven models trained on historical data may become progressively outdated. The presented residual-
751 based approach (quantifying MB) enables early detection of such divergence, offering a method for
752 identifying when ~~re-training~~ model retraining or reparameterization is needed to maintain predictive
753 reliability under non-stationary conditions.

754 5. Summary and conclusions

755 The ~~temporal~~ Temporal variations in the water content of the topsoil ~~define the amount of plant available~~
756 control near-surface hydraulic conditions, infiltration, evaporation, and gas exchange, thereby shaping
757 soil water and oxygen supply, affecting ecosystem functions ~~dynamics~~ and physical soil health
758 status ~~functioning~~. Reliable information on soil water content dynamics in response to atmospheric
759 conditions is thus essential to detect and mitigate critical ~~conditions~~ changes in soil hydraulic behaviour.

760 This response depends on soil hydraulic properties that are traditionally characterized by a time-
761 invariant and unambiguous relationship between matric potential, water content, and hydraulic
762 conductivity as deduced from small-scale lab experiments. In this study, we developed and applied a
763 feed-forward neural network combined with seasonal trend analysis of climatic time series to quantify
764 the soil water content response function after an extreme drought in summer 2018 in Germany. By

765 analysing the time series of topsoil water content measured at two lysimeter stations of the TERENO
766 SOILCan network, we summarize the conclusion on the soil water content response function as follows:

- 767 • 50% of the lysimeters showed changes in soil water content dynamics after the dry summer
768 2018 ~~without recovery until the year 2023.~~
- 769 • The other half showed a resilient behaviour, and the soil water content response function was
770 not permanently changed.
- 771 • The changes in soil water content response function were manifested as (i) temporal trends in
772 prediction error (mean bias) and (ii) shifts in the soil water characteristics function.
- 773 • The soil water content response function is adapted to climatic conditions as manifested by (i)
774 smallest changes in lysimeters that were not translocated and (ii) decreased model performance
775 for applications of a response function that was determined for another climate.
- 776 • Good model performance as expressed by high Nash-~~Shutcliff Efficiency~~ ~~Sutcliffe efficiency~~
777 values does not correspond to stable soil water content response function that was only detected
778 by temporal trends in error metrics.

779 The study revealed that ~~extreme climatic~~ ~~intense drought~~ events can ~~permanently change the~~ ~~induce~~
780 ~~lasting changes in~~ soil hydraulic properties, but the ~~lack~~ ~~degree~~ of resilience depends on ~~the~~ ~~both~~ soil
781 ~~type~~ and ~~the~~ climatic conditions. We argue that ~~the response depends on the~~ ~~soils which developed under~~
782 ~~a broader~~ range of climatic conditions ~~experienced in the past that allowed adaptation of~~ ~~may possess~~
783 soil ~~structural~~ hydraulic properties: ~~that enhance resilience to subsequent drought, and that this inherited~~
784 ~~behaviour persists after translocation to a new climatic regime.~~ Because the presented model framework
785 ~~(i)~~ ~~does~~ (i) not aim to predict successfully time series in water content and (ii) ~~does~~ only require
786 categorical water content information ('stable', 'resilient', 'changed'), it can be applied to larger scale
787 using remote sensing data that do not provide accurate soil water content values but reliable trends,
788 enabling to detect changes in hydraulic behaviour at the ecosystem scale.

789 **Author contributions**

790 NA, AC, and PL designed the study. NA and PL conducted the research. NA developed the model and
791 wrote the code. NA and PL prepared the manuscript with contributions of all co-authors. JG and RG
792 provided and quality-controlled the lysimeter data.

793 **Acknowledgements**

794 We acknowledge the support of ~~the TERENO- and SOILCan-network that, which~~ were funded by the
795 Helmholtz Association (HGF) and the Federal Ministry of Education and Research (BMBF). ~~We thank~~
796 ~~Ferdinand Engels, Robert Lüdtkke, Werner Küpper, Ines Merbach, Philipp Meulendick, and Syliva~~
797 ~~Schmögner for the instrument operation and data processing at both sites. We also thank Hans Jörg~~
798 ~~Vogel for his constructive feedback and insightful comments on the manuscript. Nedal Aqel~~
799 ~~acknowledges the utilization of ChatGPT to enhance coherence within certain sections of the paper.,~~
800 Germany).

801 We would like to thank Ines Merbach, Sylvia Schmögner, Werner Küpper, Philipp Meulendick,
802 Ferdinand Engels, Antonio Voss, Leander Fürst and Rainer Harms for their kind support at the lysimeter
803 stations in Bad Lauchstädt and Selhausen. We thank Hans-Jörg Vogel for his constructive feedback and
804 insightful comments on the manuscript.

805 **Financial support**

806 This research is part of the project AI4SoilHealth of the European Union's Horizon research and
807 innovation programme (grant agreement No. 101086179). This work has received funding from the
808 Swiss State Secretariat for Education, Research and Innovation (SERI).

809

810 **References**

- 811 Allen, R. G., Pereira, L. S., Raes, D., and Smith, M.: Crop evapotranspiration – Guidelines for
812 computing crop water requirements, FAO Irrigation and Drainage Paper 56, Food and
813 Agriculture Organization of the United Nations, Rome, 300 pp., 2006.
- 814 Aqel, N., Reusser, L., Margreth, S., Carminati, A., and Lehmann, P.: Prediction of hysteretic
815 matric potential dynamics using artificial intelligence: application of autoencoder neural
816 networks, *Geosci. Model Dev.*, 17, 6949–6966, <https://doi.org/10.5194/gmd-17-6949-2024>,
817 2024.
- 818 Blöschl, G., Bierkens, M. F. P., Chambel, A., Cudennec, C., Destouni, G., Fiori, A., Kirchner, J. W.,
819 McDonnell, J. J., Savenije, H. H. G., Sivapalan, M., Stumpp, C., Toth, E., Volpi, E., Carr, G.,
820 Lupton, C., Salinas, J., Széles, B., Viglione, A., Aksoy, H., and Zhang, Y.: Twenty-three unsolved
821 problems in hydrology (UPH) – a community perspective, *Hydrol. Sci. J.*, 64, 1141–1158,
822 <https://doi.org/10.1080/02626667.2019.1620507>, 2019.
- 823 Boergens, E., Güntner, A., Sips, M., Schwatke, C., and Dobsław, H.: Interannual variations of
824 terrestrial water storage in the East African Rift region, *Hydrol. Earth Syst. Sci.*, 28, 4733–4754,
825 <https://doi.org/10.5194/hess-28-4733-2024>, 2024.
- 826 Bogena, H. R., Huisman, J. A., Güntner, A., Hübner, C., Kusche, J., Jonard, F., Vey, S., and
827 Vereecken, H.: Emerging methods for noninvasive sensing of soil moisture dynamics from field
828 to catchment scale: a review, *WIREs Water*, 2, 635–647, <https://doi.org/10.1002/wat2.1097>,
829 2015.
- 830 Brocca, L., Melone, F., Moramarco, T., Wagner, W., Naeimi, V., Bartalis, Z., and Hasenauer, S.:
831 Improving runoff prediction through the assimilation of the ASCAT soil moisture product,
832 *Hydrol. Earth Syst. Sci.*, 14, 1881–1893, <https://doi.org/10.5194/hess-14-1881-2010>, 2010.
- 833 Cleveland, R. B., Cleveland, W. S., McRae, J. E., and Terpenning, I.: STL: A seasonal-trend
834 decomposition procedure based on Loess, *J. Off. Stat.*, 6, 3–73, 1990.
- 835 Detty, J. M. and McGuire, K. J.: Threshold changes in storm runoff generation at a till-mantled
836 headwater catchment, *Water Resour. Res.*, 46, W07525,
837 <https://doi.org/10.1029/2009WR008102>, 2010.
- 838 Deutscher Wetterdienst (DWD) Climate Data Center (CDC): Historical daily precipitation data,
839 station Leipzig/Halle (ID 2932), available at: <https://www.dwd.de/cdc> (last access: 28 August
840 2025), 2025.
- 841 ~~Ehrhardt, A., Groh, J., and Gerke, H. H.: Effects of different climatic conditions on soil water
842 storage patterns, *Hydrol. Earth Syst. Sci.*, 29, 313–334, [https://doi.org/10.5194/hess-29-313-](https://doi.org/10.5194/hess-29-313-2025)
843 ~~2025~~, 2025.~~
- 844 Fatichi, S., Or, D., Walko, R., Vereecken, H., Young, M. H., Ghezzehei, T. A., Hengl, T., Kollet, S.,
845 Agam, N., and Avissar, R.: Soil structure is an important omission in Earth system models, *Nat.*
846 *Commun.*, 11, 522, <https://doi.org/10.1038/s41467-020-14411-z>, 2020.
- 847 Fu, Z., Hu, W., Beare, M., Thomas, S., Carrick, S., Dando, J., Langer, S., Müller, K., Baird, D., and
848 Lilburne, L.: Land use effects on soil hydraulic properties and the contribution of soil organic
849 carbon, *J. Hydrol.*, 602, 126741, <https://doi.org/10.1016/j.jhydrol.2021.126741>, 2021.

850 Groh, J., Diamantopoulos, E., Duan, X., Ewert, F., Heinlein, F., Herbst, M., Holbak, M., Kamali, B.,
851 Kersebaum, K.-C., Kuhnert, M., Nendel, C., Priesack, E., Steidl, J., Sommer, M., Pütz, T.,
852 Vanderborght, J., Vereecken, H., Wallor, E., Weber, T. K. D., and Gerke, H. H.: Same soil,
853 different climate: crop model intercomparison on translocated lysimeters, *Vadose Zone J.*, 21,
854 e20202, <https://doi.org/10.1002/vzj2.20202>, 2022.

855 Groh, J., Vanderborght, J., Pütz, T., Vogel, H.-J., Gründling, R., Rupp, H., Rahmati, M., Sommer,
856 M., Vereecken, H., and Gerke, H. H.: Responses of soil water storage and crop water use
857 efficiency to changing climatic conditions: a lysimeter-based space-for-time approach, *Hydrol.*
858 *Earth Syst. Sci.*, 24, 1211–1225, <https://doi.org/10.5194/hess-24-1211-2020>, 2020.

859 Hannes, M., Wollschläger, U., Wöhling, T., and Vogel, H.-J.: Revisiting hydraulic hysteresis based
860 on long-term monitoring of hydraulic states in lysimeters, *Water Resour. Res.*, 52, 3847–3865,
861 <https://doi.org/10.1002/2015WR018319>, 2016.

862 Hari, V., Rakovec, O., Markonis, Y., Hanel, M., and Kumar, R.: Increased future occurrences of
863 the exceptional 2018–2019 Central European drought under global warming, *Sci. Rep.*, 10,
864 12207, <https://doi.org/10.1038/s41598-020-68872-9>, 2020.

865 Herbrich, M. and Gerke, H. H.: Scales of water retention dynamics observed in eroded Luvisols
866 from an arable postglacial soil landscape, *Vadose Zone J.*, 16, 1–12,
867 <https://doi.org/10.2136/vzj2017.01.0003>, 2017.

868 [Hirmas, D. R., Giménez, D., Nemes, A., Kerry, R., Brunsell, N. A., and Wilson, C. J.: Climate-](https://doi.org/10.1038/s41586-018-0463-x)
869 [induced changes in continental-scale soil macroporosity may intensify water cycle, *Nature*, 561,](https://doi.org/10.1038/s41586-018-0463-x)
870 [100–103, <https://doi.org/10.1038/s41586-018-0463-x>, 2018.](https://doi.org/10.1038/s41586-018-0463-x)

871 [Holling, C. S.: Resilience and stability of ecological systems, IIASA Research Report RR-73-003](https://pure.iiasa.ac.at/id/eprint/26/1/RP-73-003.pdf)
872 [\(Reprint\), IIASA, Laxenburg, Austria, reprinted from *Annual Review of Ecology and Systematics*,](https://pure.iiasa.ac.at/id/eprint/26/1/RP-73-003.pdf)
873 [4, 1–23, <https://pure.iiasa.ac.at/id/eprint/26/1/RP-73-003.pdf>, 1973.](https://pure.iiasa.ac.at/id/eprint/26/1/RP-73-003.pdf)

874 Hrachowitz, M., Savenije, H. H. G., Blöschl, G., McDonnell, J. J., Sivapalan, M., Pomeroy, J. W.,
875 Arheimer, B., Blume, T., Clark, M. P., Ehret, U., Fenicia, F., Freer, J. E., Gelfan, A., Gupta, H. V.,
876 Hughes, D. A., Hut, R. W., Montanari, A., Pande, S., Tetzlaff, D., and Cudennec, C.: A decade of
877 Predictions in Ungauged Basins (PUB) – a review, *Hydrol. Sci. J.*, 58, 1198–1255,
878 <https://doi.org/10.1080/02626667.2013.803183>, 2013.

879 Jarvis, N. J., ~~Bever~~Couchenev, E., Lewan, E., Klöffel, T., Meurer, K. J., H. E., Keller, T., and Larsbo,
880 M., ~~van Genuchten, M. T., Vereecken, H., and Vogel, H. J.~~: Interactions between soil structure
881 dynamics, hydrological processes and organic matter cycling: a new soil–crop model, *Eur. J.*
882 *Soil Sci.*, 75, e13455, <https://doi.org/10.1111/ejss.13455>, 2024.

883 [Kingma, D. P., and Ba, J.: Adam: A method for stochastic optimization, *Proceedings of the*](https://arxiv.org/abs/1412.6980)
884 [*International Conference on Learning Representations \(ICLR\)*, 2015,](https://arxiv.org/abs/1412.6980)
885 <https://arxiv.org/abs/1412.6980>, 2015.

886 [Klöffel, T., Barron, J., Nemes, A., Giménez, D., and Jarvis, N. J.: Soil, climate, time and site](https://doi.org/10.1016/j.geoderma.2024.116772)
887 [factors as drivers of soil structure evolution in agricultural soils from a temperate-boreal](https://doi.org/10.1016/j.geoderma.2024.116772)
888 [region, *Geoderma*, 442, 116772, <https://doi.org/10.1016/j.geoderma.2024.116772>, 2024.](https://doi.org/10.1016/j.geoderma.2024.116772)

889 Kratzert, F., Klotz, D., Shalev, G., Klambauer, G., Hochreiter, S., and Nearing, G. S.: Towards
890 learning universal, regional, and local hydrological behaviours via machine learning applied to

891 large-sample datasets, *Hydrol. Earth Syst. Sci.*, 23, 5089–5110, [https://doi.org/10.5194/hess-](https://doi.org/10.5194/hess-23-5089-2019)
892 23-5089-2019, 2019.

893 [Kuzyakov, Y., and Zamanian, K.: Reviews and syntheses: Agropedogenesis – humankind as the](https://doi.org/10.5194/bg-16-4783-2019)
894 [sixth soil-forming factor and attractors of agricultural soil degradation, *Biogeosciences*, 16,](https://doi.org/10.5194/bg-16-4783-2019)
895 [4783–4803, <https://doi.org/10.5194/bg-16-4783-2019>, 2019.](https://doi.org/10.5194/bg-16-4783-2019)

896 Lehmann, P., Bickel, S., Wei, Z., and Or, D.: Physical constraints for improved soil hydraulic
897 parameter estimation by pedotransfer functions, *Water Resour. Res.*, 56, e2019WR025963,
898 <https://doi.org/10.1029/2019WR025963>, 2020.

899 Liu, J., Hughes, D., Rahmani, F., Lawson, K., and Shen, C.: Evaluating a global soil moisture
900 dataset from a multitask model (GSM3 v1.0) with potential applications for crop threats,
901 *Geosci. Model Dev.*, 16, 1553–1567, <https://doi.org/10.5194/gmd-16-1553-2023>, 2023.

902 Liu, J., Rahmani, F., Lawson, K., and Shen, C.: A multiscale deep learning model for soil moisture
903 integrating satellite and in situ data, *Geophys. Res. Lett.*, 49, e2021GL096847,
904 <https://doi.org/10.1029/2021GL096847>, 2022.

905 Liu, Y. Y., Parinussa, R. M., Dorigo, W. A., De Jeu, R. A. M., Wagner, W., van Dijk, A. I. J. M.,
906 McCabe, M. F., and Evans, J. P.: Developing an improved soil moisture dataset by blending
907 passive and active microwave satellite-based retrievals, *Hydrol. Earth Syst. Sci.*, 15, 425–436,
908 <https://doi.org/10.5194/hess-15-425-2011>, 2011.

909 Lu, L., Shin, Y., Su, Y., and Karniadakis, G. E.: Dying ReLU and initialization: theory and numerical
910 examples, *Commun. Comput. Phys.*, 28, 1671–1706, [https://doi.org/10.4208/cicp.OA-2020-](https://doi.org/10.4208/cicp.OA-2020-0165)
911 0165, 2020.

912 Melsen, L. A. and Guse, B.: Climate change impacts model parameter sensitivity – implications
913 for calibration strategy and model diagnostic evaluation, *Hydrol. Earth Syst. Sci.*, 25, 1307–
914 1332, <https://doi.org/10.5194/hess-25-1307-2021>, 2021.

915 Milly, P. C. D., Betancourt, J., Falkenmark, M., Hirsch, R. M., Kundzewicz, Z. W., Lettenmaier, D.
916 P., and Stouffer, R. J.: Stationarity is dead: whither water management?, *Science*, 319, 573–
917 574, <https://doi.org/10.1126/science.1151915>, 2008.

918 Montanari, A., Young, G., Savenije, H. H. G., Hughes, D., Wagener, T., Ren, L.-L., Koutsoyiannis,
919 D., Cudennec, C., Toth, E., Grimaldi, S., Blöschl, G., Sivapalan, M., Beven, K., Gupta, H., Hipsey,
920 B., Schaeffli, B., Arheimer, B., Boegh, E., Schymanski, S. J., and Belyaev, V.: “Panta Rhei—
921 Everything Flows”: change in hydrology and society—The IAHS Scientific Decade 2013–2022,
922 *Hydrol. Sci. J.*, 58, 1256–1275, <https://doi.org/10.1080/02626667.2013.809088>, 2013.

923 Montesinos López, O. A., Montesinos López, A., and Crossa, J.: Fundamentals of artificial neural
924 networks and deep learning, in: *Multivariate Statistical Machine Learning Methods for*
925 *Genomic Prediction*, Springer International Publishing, Cham, 379–425,
926 https://doi.org/10.1007/978-3-030-89010-0_10, 2022.

927 Moriasi, D. N., Arnold, J. G., Van Liew, M. W., Bingner, R. L., Harmel, R. D., and Veith, T. L.:
928 Model evaluation guidelines for systematic quantification of accuracy in watershed
929 simulations, *Trans. ASABE*, 50, 885–900, <https://doi.org/10.13031/2013.23153>, 2007.

930 Moriasi, D. N., Gitau, M. W., Pai, N., and Daggupati, P.: Hydrologic and water quality models:
931 Performance measures and evaluation criteria, *Trans. ASABE*, **58**, 1763–1785, 2015.
932 <https://web.ics.purdue.edu/~mgitau/pdf/Moriasi%20et%20al%202015.pdf>

933 Mosavi, A., Ozturk, P., and Chau, K.-W.: Flood prediction using machine learning models:
934 literature review, *Water*, **10**, 1536, <https://doi.org/10.3390/w10111536>, 2018.

935 Nash, J. E. and Sutcliffe, J. V.: River flow forecasting through conceptual models part I — A
936 discussion of principles, *J. Hydrol.*, **10**, 282–290, [https://doi.org/10.1016/0022-1694\(70\)90255-](https://doi.org/10.1016/0022-1694(70)90255-6)
937 [6](https://doi.org/10.1016/0022-1694(70)90255-6), 1970.

938 Nearing, G. S., Kratzert, F., Sampson, A. K., Pelissier, C. S., Klotz, D., Frame, J. M., Prieto, C., and
939 Gupta, H. V.: What role does hydrological science play in the age of machine learning?, *Water*
940 *Resour. Res.*, **57**, e2020WR028091, <https://doi.org/10.1029/2020WR028091>, 2021.

941 O., S. and Orth, R.: Global soil moisture data derived through machine learning trained with in-
942 situ measurements, *Sci. Data*, **8**, 170, <https://doi.org/10.1038/s41597-021-00964-1>, 2021.

943 Pütz, T., Kiese, R., Wollschläger, U., Groh, J., Rupp, H., Zacharias, S., Priesack, E., Gerke, H. H.,
944 Gasche, R., Bens, O., Borg, E., Baessler, C., Kaiser, K., Herbrich, M., Munch, J.-C., Sommer, M.,
945 Vogel, H.-J., Vanderborght, J., and Vereecken, H.: TERENO-SOILCan: a lysimeter-network in
946 Germany observing soil processes and plant diversity influenced by climate change, *Environ.*
947 *Earth Sci.*, **75**, 1242, <https://doi.org/10.1007/s12665-016-6031-5>, 2016.

948 [Quintana, J. R., Martín-Sanz, J. P., Valverde-Asenjo, I., and Molina, J. A.: Drought differently](https://doi.org/10.1016/j.catena.2022.106871)
949 [destabilizes soil structure in a chronosequence of abandoned agricultural lands, *Catena*, **222**,](https://doi.org/10.1016/j.catena.2022.106871)
950 [106871, https://doi.org/10.1016/j.catena.2022.106871, 2023.](https://doi.org/10.1016/j.catena.2022.106871)

951 Reichstein, M., Camps-Valls, G., Stevens, B., Jung, M., Denzler, J., Carvalhais, N., and Prabhat:
952 Deep learning and process understanding for data-driven Earth system science, *Nature*, **566**,
953 **195–204**, <https://doi.org/10.1038/s41586-019-0912-1>, 2019.

954 Robinson, D. A., Jones, S. B., Lebron, I., Reinsch, S., Domínguez, M. T., Smith, A. R., Jones, D. L.,
955 Marshall, M. R., and Emmett, B. A.: Experimental evidence for drought induced alternative
956 stable states of soil moisture, *Sci. Rep.*, **6**, 20018, <https://doi.org/10.1038/srep20018>, 2016.

957 [Robinson, D. A., Hopmans, J. W., Filipović, V., van der Ploeg, M., Lebron, I., Jones, S. B., Reinsch,](https://doi.org/10.1111/gcb.14626)
958 [S., Jarvis, N., and Tuller, M.: Global environmental changes impact soil hydraulic functions](https://doi.org/10.1111/gcb.14626)
959 [through biophysical feedbacks, *Glob. Change Biol.*, **25**, 1895–1904,](https://doi.org/10.1111/gcb.14626)
960 [https://doi.org/10.1111/gcb.14626, 2019.](https://doi.org/10.1111/gcb.14626)

961 [Robinson, D. A., Nemes, A., Reinsch, S., Radbourne, A., Bentley, L., and Keith, A. M.: Global](https://doi.org/10.1016/j.scitotenv.2022.158506)
962 [meta-analysis of soil hydraulic properties on the same soils with differing land use, *Sci. Total*](https://doi.org/10.1016/j.scitotenv.2022.158506)
963 [Environ., **852**, 158506, <https://doi.org/10.1016/j.scitotenv.2022.158506>, 2022.](https://doi.org/10.1016/j.scitotenv.2022.158506)

964 [Sainju, U. M., Liptzin, D., and Jabro, J. D.: Relating soil physical properties to other soil](https://doi.org/10.1038/s41598-022-26619-8)
965 [properties and crop yields, *Sci. Rep.*, **12**, 22025, <https://doi.org/10.1038/s41598-022-26619-8>,](https://doi.org/10.1038/s41598-022-26619-8)
966 [2022.](https://doi.org/10.1038/s41598-022-26619-8)

967 Seneviratne, S. I., Corti, T., Davin, E. L., Hirschi, M., Jaeger, E. B., Lehner, I., Orlowsky, B., and
968 Teuling, A. J.: Investigating soil moisture–climate interactions in a changing climate: a review,
969 *Earth-Sci. Rev.*, **99**, 125–161, <https://doi.org/10.1016/j.earscirev.2010.02.004>, 2010.

970 Shen, C., Laloy, E., Elshorbagy, A., Albert, A., Bales, J., Chang, F.-J., Ganguly, S., Hsu, K.-L., Kifer,
971 D., Fang, Z., Fang, K., Li, D., Li, X., and Tsai, W.-P.: HESS Opinions: Incubating deep-learning-
972 powered hydrologic science advances as a community, *Hydrol. Earth Syst. Sci.*, 22, 5639–5656,
973 <https://doi.org/10.5194/hess-22-5639-2018>, 2018.

974 Sun, W., Zhou, S., Yu, B., Zhang, Y., Keenan, T., and Fu, B.: Soil moisture–atmosphere
975 interactions drive terrestrial carbon–water trade-offs, *Commun. Earth Environ.*, 6, 169,
976 <https://doi.org/10.1038/s43247-025-02145-z>, 2025.

977 Tromp-van Meerveld, H. J. and McDonnell, J. J.: Threshold relations in subsurface stormflow: 1.
978 A 147-storm analysis of the Panola hillslope, *Water Resour. Res.*, 42, W02410,
979 <https://doi.org/10.1029/2004WR003778>, 2006.

980 Uber, M., Vandervaere, J.-P., Zin, I., Braud, I., Heistermann, M., Legoût, C., Molinié, G., and
981 Nord, G.: How does initial soil moisture influence the hydrological response? A case study from
982 southern France, *Hydrol. Earth Syst. Sci.*, 22, 6127–6146, [https://doi.org/10.5194/hess-22-](https://doi.org/10.5194/hess-22-6127-2018)
983 [6127-2018](https://doi.org/10.5194/hess-22-6127-2018), 2018.

984 Vaze, J., Post, D. A., Chiew, F. H. S., Perraud, J.-M., Viney, N. R., and Teng, J.: Climate non-
985 stationarity – validity of calibrated rainfall–runoff models for use in climate change studies, *J.*
986 *Hydrol.*, 394, 447–457, <https://doi.org/10.1016/j.jhydrol.2010.09.018>, 2010.

987 Vereecken, H., Amelung, W., Bauke, S. L., Bogaen, H., Brüggemann, N., Montzka, C.,
988 Vanderborght, J., Bechtold, M., Blöschl, G., Carminati, A., Javaux, M., Konings, A. G., Kusche, J.,
989 Neuweiler, I., Or, D., Steele-Dunne, S., Verhoef, A., Young, M., and Zhang, Y.: Soil hydrology in
990 the Earth system, *Nat. Rev. Earth Environ.*, 3, 573–587, [https://doi.org/10.1038/s43017-022-](https://doi.org/10.1038/s43017-022-00324-6)
991 [00324-6](https://doi.org/10.1038/s43017-022-00324-6), 2022.

992 Vereecken, H., Huisman, J. A., Bogaen, H., Vanderborght, J., Vrugt, J. A., and Hopmans, J. W.:
993 On the value of soil moisture measurements in vadose zone hydrology: a review, *Water*
994 *Resour. Res.*, 44, W00D06, <https://doi.org/10.1029/2008WR006829>, 2008.

995 Wankmüller, F. J. P., Delval, L., Lehmann, P., Baur, M. J., Cecere, A., Wolf, S., Or, D., Javaux, M.,
996 and Carminati, A.: Global influence of soil texture on ecosystem water limitation, *Nature*, 635,
997 631–638, <https://doi.org/10.1038/s41586-024-08089-2>, 2024.

998 Western, A. W. and Grayson, R. B.: The Tarrawarra data set: soil moisture patterns, soil
999 characteristics, and hydrological flux measurements, *Water Resour. Res.*, 34, 2765–2768,
1000 <https://doi.org/10.1029/98WR01833>, 1998.

1001 Xoplaki, E., Ellsäßer, F., Grieger, J., Nissen, K. M., Pinto, J. G., Augenstein, M., Chen, T.-C., and
1002 Wolf, F.: Compound events in Germany in 2018: drivers and case studies, *Nat. Hazards Earth*
1003 *Syst. Sci.*, 25, 541–564, <https://doi.org/10.5194/nhess-25-541-2025>, 2025.

1004 Zehe, E. and Blöschl, G.: Predictability of hydrologic response at the plot and catchment scales:
1005 role of initial conditions, *Water Resour. Res.*, 40, W10240,
1006 <https://doi.org/10.1029/2003WR002869>, 2004.

1007 Šimůnek, J., van Genuchten, M. T., and Šejna, M.: Recent developments and applications of the
1008 HYDRUS computer software packages, *Vadose Zone J.*, 15, 1–25,
1009 <https://doi.org/10.2136/vzj2016.04.0033>, 2016.

1010